THE JOURNAL OF BIOLOGICAL CHEMISTRY VOL. 291, NO. 12, pp. 6396–6411, March 18, 2016

Ty1 Integrase Interacts with RNA Polymerase III-specific Subcomplexes to Promote Insertion of Ty1 Elements Upstream of Polymerase (Pol) III-transcribed Genes*

Received for publication, August 26, 2015, and in revised form, January 11, 2016 Published, JBC Papers in Press, January 21, 2016, DOI 10.1074/jbc.M115.686840

Stephanie Cheung[‡§], Lina Ma[§], Patrick H. W. Chan[¶], Hui-Lan Hu[‖], Thibault Mayor[‡¶1], Hung-Ta Chen[‖], and Vivien Measday[‡§2]

From the [‡]Department of Biochemistry and Molecular Biology, [§]Wine Research Centre, and [¶]Centre for High-Throughput Biology, University of British Columbia, Vancouver, British Columbia V6T 1Z4, Canada and [‖]Institute of Molecular Biology, Academia Sinica, Taipei, Taiwan 115

Retrotransposons are eukaryotic mobile genetic elements that transpose by reverse transcription of an RNA intermediate and are derived from retroviruses. The Ty1 retrotransposon of *Saccharomyces cerevisiae* belongs to the Ty1/Copia superfamily, which is present in every eukaryotic genome. Insertion of Ty1 elements into the *S. cerevisiae* genome, which occurs upstream of genes transcribed by RNA Pol III, requires the Ty1 element-encoded integrase (IN) protein. Here, we report that Ty1-IN interacts *in vivo* and *in vitro* with RNA Pol III-specific subunits to mediate insertion of Ty1 elements upstream of Pol III-transcribed genes. Purification of Ty1-IN from yeast cells followed by mass spectrometry (MS) analysis identified an enrichment of peptides corresponding to the Rpc82/34/31 and Rpc53/37 Pol III-specific subcomplexes. GFP-Trap purification of multiple GFP-tagged RNA Pol III subunits from yeast extracts revealed that the majority of Pol III subunits co-purify with Ty1-IN but not two other complexes required for Pol III transcription, transcription initiation factors (TF) IIIB and IIIC. *In vitro* binding studies with bacterially purified RNA Pol III proteins demonstrate that Rpc31, Rpc34, and Rpc53 interact directly with Ty1-IN. Deletion of the N-terminal 280 amino acids of Rpc53 abrogates insertion of Ty1 elements upstream of the hot spot *SUF16* tRNA locus and abolishes the interaction of Ty1-IN with Rpc37. The Rpc53/37 complex therefore has an important role in targeting Ty1-IN to insert Ty1 elements upstream of Pol III-transcribed genes.

Retrotransposons are transposable elements that share similarities to retroviruses, although they lack an infectious phase in their life cycle. The genome of the yeast *Saccharomyces cerevisiae* contains five families of Ty retrotransposons (Ty1–5) of which Ty1 is the most abundant (1). Ty1–5 are long terminal repeat retrotransposons because each ~6-kilobase pair (kbp) Ty element is flanked by a ~330-base pair (bp) direct repeat sequence. The remainder of the element comprises both TyA and TyB open reading frames (ORFs), analogous to retroviral Gag and Pol, respectively. Gag encodes the structural elements of the viral coat protein, whereas Pol is a polyprotein that is cleaved to generate a protease (PR),[3] IN, and reverse transcriptase (RT) (2, 3). Ty elements propagate by reverse transcribing their RNA into cDNA in virus-like particles and incorporating the cDNA into a preintegration complex with Ty-IN, which is imported into the nucleus for targeting into the genome. Ty1, Ty2, and Ty4 elements insert within a ~1-kbp window upstream of genes transcribed by RNA Pol III such as tRNA genes, and Ty1 insertion is blocked by mutations in the Pol III promoter, suggesting that active Pol III transcription is required for Ty1 element insertion (4, 5). Ty3 elements insert within a few bp of the RNA Pol III transcription start site, and an interaction between Ty3-IN and the TFIIIB factor Brf1 is sufficient to target Ty3 to Pol III transcription start sites *in vitro* (6–8). Ty5, however, interacts with Sir4 to mediate insertion into the silenced regions of the genome such as the silent mating type loci and telomeric regions (9, 10). Ty1 insertion occurs with a periodicity of ~80 bp and is coincident with nucleosome positioning (11–14). Disruption of the chromatin structure upstream of tRNA genes disrupts the periodicity of Ty1 element insertion but not integration site selection (15, 16). Although many nuclear factors have been identified that either restrict or promote Ty1 integration, proteins that physically interact with Ty1-IN to target it upstream of Pol III-transcribed genes have remained elusive until recently (17–22). Ty1-IN interacts with separase, a protein that cleaves the cohesin complex to mediate separation of sister chromatids (23). However, despite the fact that separase mutants have reduced and cohesin mutants have increased Ty1 insertion frequency, no change in targeting specificity was demonstrated (23). Recently, a yeast two-hybrid screen using the RNA Pol III AC40 subunit as bait identified an interaction with Ty1-IN (24). Replacing the *S. cerevisiae* AC40 subunit with *Schizosaccharomyces pombe* AC40 disrupted the interaction with Ty1-IN and

* The authors declare that they have no conflicts of interest with the contents of this article.

[1] Supported by the Canadian Institutes of Health Research (CIHR) and Michael Smith Foundation for Health Research new investigator awards and Natural Sciences and Engineering Research Council of Canada (NSERC) Discovery (DG) Grant RGPIN 355729-11.

[2] Supported by CIHR Grant HOP-131559 and NSERC DG Grant RPGIN 326924-11. To whom correspondence should be addressed: Wine Research Centre, Rm. 325, 2205 East Mall, University of British Columbia, Vancouver, British Columbia V6T 1Z4, Canada. Tel.: 604-827-5744; Fax: 604-822-5143; E-mail: vmeasday@mail.ubc.ca.

[3] The abbreviations used are: PR, protease; Pol, polymerase; IN, integrase; TF, transcription initiation factor; RT, reverse transcriptase; IP, immunoprecipitation; SC, synthetic complete medium; MBP, maltose-binding protein; Chr, chromosome(s); qPCR, quantitative PCR; RQ, relative quantity; NLS, nuclear localization signal; ts, temperature-sensitive; AI, artificial intron.

TABLE 1
Yeast strains used in this study

Strain	Genotype	Ref.
BY4741	MATa *his3Δ1 leu2Δ0 ura3Δ0 met15Δ0*	76
LV1491	MATα *ura3-167 his3Δ200 Ty1his3AI-242 rpc40Δ::hphMX pCEN AmpR URA3 TetO7-RPC40*	24
LV1492	MATα *ura3-167 his3Δ200 Ty1his3AI-242 rpc40Δ::hphMX pCEN AmpR URA3 TetO7-Rpc40+* (*S. pombe*)	24
Y7092	MATα *can1Δ::STE2pr-Sp_his5 lyp1Δ his3Δ1 leu2Δ0 ura3Δ0 met15Δ0*	77
YKH638	MATa *his3Δ1 leu2Δ0 lys2Δ0 met15Δ ura3Δ0 spt3::KanMX6*	78
YLM2119A	MATa *his3Δ1 leu2Δ0 met15Δ ura3Δ0 trp::KanMX6 RPC82-GFP::HIS3*	This study
YLM2120	MATa *his3Δ1 leu2Δ0 lys2Δ0 met15Δ ura3Δ0 RPC34-HA::HIS3*	This study
YLM2124	MATa *his3Δ1 leu2Δ0 lys2Δ0 met15Δ ura3Δ0 RPC25-HA::HIS3*	This study
YM2371	MATa *his3Δ1 leu2Δ0 met15Δ ura3Δ0 RPC82-GFP::HIS3*	42
YM2346	MATa *his3Δ1 leu2Δ0 ura3Δ0 met15Δ0 rpo31-698::kanMX6*	52
YM2347	MATa *his3Δ1 leu2Δ0 ura3Δ0 met15Δ0 rpc40-V78R::kanMX6*	52
YM2348	MATa *his3Δ1 leu2Δ0 ura3Δ0 met15Δ0 rpc34-1::kanMX6*	52
YM2367	MATa *his3Δ1 leu2Δ0 met15Δ ura3Δ0 RPC17-GFP::HIS3*	42
YM2369	MATa *his3Δ1 leu2Δ0 met15Δ ura3Δ0 MAF1-GFP::HIS3*	42
YM2370	MATa *his3Δ1 leu2Δ0 met15Δ ura3Δ0 RPC160-GFP::HIS3*	42
YM2372	MATa *his3Δ1 leu2Δ0 met15Δ ura3Δ0 RPB2-GFP::HIS3*	42
YM2374	MATa *his3Δ1 leu2Δ0 met15Δ ura3Δ0 RPC40-GFP::HIS3*	42
YM2447	MATα *ade2::his3G his3Δ200 leu2Δ0 met15Δ0 lys2Δ0 trp1Δ63 ura3Δ0* [*C53::KanMX4*] *pRPC53-WT*/*pRS315*	36
YM2448	MATα *ade2::his3G his3Δ200 leu2Δ0 met15Δ0 lys2Δ0 trp1Δ63 ura3Δ0* [*C53::KanMX4*] *pRPC53Δ* (*11–40*)/pRS315	36
YM2449	MATα *ade2::his3G his3Δ200 leu2Δ0 met15Δ0 lys2Δ0 trp1Δ63 ura3Δ0* [*C53::KanMX4*] *pRPC53Δ* (*316–350*)/pRS315	36
YM2450	MATα *ade2::his3G his3Δ200 leu2Δ0 met15Δ0 lys2Δ0 trp1Δ63 ura3Δ0* [*C53::KanMX4*] *pRPC53Δ* (*2–280*)/pRS315	36
YSC16	MATa *his3Δ1 leu2Δ0 met15Δ ura3Δ0 RPO21-GFP::HIS3*	42
YSC17	MATa *his3Δ1 leu2Δ0 met15Δ ura3Δ0 RPC128-GFP::HIS3*	42
YSC18	MATa *his3Δ1 leu2Δ0 met15Δ ura3Δ0 RPB6-GFP::HIS3*	42
YSC19	MATa *his3Δ1 leu2Δ0 met15Δ ura3Δ0 RPC19-GFP::HIS3*	42
YSC42	MATa *his3Δ1 leu2Δ0 met15Δ ura3Δ0 BRF1-GFP::HIS3*	42
YSC43	MATa *his3Δ1 leu2Δ0 met15Δ ura3Δ0 BDP1-GFP::HIS3*	42
YSC44	MATa *his3Δ1 leu2Δ0 met15Δ ura3Δ0 TFC1-GFP::HIS3*	42
YSC45	MATa *his3Δ1 leu2Δ0 met15Δ ura3Δ0 TFC3-GFP::HIS3*	42
YSC47	MATa *his3Δ1 leu2Δ0 met15Δ ura3Δ0 TFC7-GFP::HIS3*	42
YSC62	MATa *his3Δ1 leu2Δ0 lys2Δ0 met15Δ ura3Δ0 RPC82-HA::HIS3*	This study
YSC97	MATa *ade2::his3G his3Δ1 leu2Δ0 met15Δ ura3Δ0 RPC17-GFP::HIS3* [*C53::KanMX4*] *pRPC53-WT*/*pRS315*	This study
YSC99	MATa *ade2::his3G his3Δ1 leu2Δ0 met15Δ ura3Δ0 RPC17-GFP::HIS3* [*C53::KanMX4*] *pRPC53* (*Δ2–280*)/*pRS315*	This study
YSC103	MATa *his3Δ1 leu2Δ0 met15Δ ura3Δ0 RPC19-GFP::HIS3* [*C53::KanMX4*] *pRPC53-WT*/*pRS315*	This study
YSC106	MATa *ade2::his3G his3Δ1 leu2Δ0 met15Δ ura3Δ0 RPC37-GFP::HIS3* [*C53::KanMX4*] *pRPC53* (*Δ2–280*)/*pRS315*	
YSC107	MATa *his3Δ1 leu2Δ0 met15Δ ura3Δ0 RPC19-GFP::HIS3* [*C53::KanMX4*] *pRPC53* (*Δ2–280*)/*pRS315*	This study
YSC109	MATa *ade2::his3G his3Δ1 leu2Δ0 met15Δ ura3Δ0 RPC37-GFP::HIS3* [*C53::KanMX4*] *pRPC53-WT*/*pRS315*	This study
YSC111	MATa *ade2::his3G his3Δ1 leu2Δ0 met15Δ ura3Δ0 RPC82-GFP::HIS3* [*C53::KanMX4*] *pRPC53-WT*/*pRS315*	This study
YSC113	MATa *ade2::his3G his3Δ1 leu2Δ0 met15Δ ura3Δ0 RPC82-GFP::HIS3* [*C53::KanMX4*] *pRPC53* (*Δ2–280*)/*pRS315*	This study

redirected Ty1 element insertion to telomeric and subtelomeric regions (24). This exciting new discovery provides significant insight into the mechanism of Ty1 element insertion. However, despite the lack of interaction between *S. pombe* AC40 and Ty1-IN, overall Ty1 mobility was not affected, suggesting that other factors could still mediate Ty1 element insertion (24).

In this study, we performed purification of Ty1-IN from yeast cells followed by MS analysis and identified an enrichment of RNA Pol III subunits in our Ty1-IN purifications. The RNA Pol III complex is a 17-subunit complex composed of a 10-subunit core with five subunits shared between all three Pols and two of the remaining five shared between Pol I and Pol III (Rpc40/AC40 and Rpc19/AC19) (25). There are two Pol III-specific subcomplexes composed of Rpc82/34/31 and Rpc53/37 and the Rpb4/7-like subcomplex containing Rpc25/17 (25). We demonstrate that multiple RNA Pol III proteins, including the Pol III-specific proteins, co-immunoprecipitate with Ty1-IN from yeast lysates. A purified RNA Pol III complex from yeast binds to Ty1-IN *in vitro* as well as *Escherichia coli* purified Rpc31, Rpc34, and Rpc53. We demonstrate that removing the N terminus of Rpc53 prevents Ty1 targeting to the *SUF16* tRNA locus and abolishes the interaction of Ty1-IN with Rpc37. Our data suggest that the Rpc53/37 Pol III-specific subcomplex is required for specific targeting of Ty1-IN upstream of Pol III-transcribed genes.

Experimental Procedures

Yeast Strain Construction—S. cerevisiae strains used in this study are listed in Table 1. All C-terminal epitope tags (GFP and HA) were generated by PCR and homologous recombination as described (26).

Plasmid Construction—Ty1-IN-S (BSC3A) was constructed by amplifying Ty1-IN from yeast genomic DNA using the following primers: OSC8, 5′-CCCCATATGAATGTCCATACAAGTGAAAGTAC-3′; OSC9, 5′-CCCCTCGAGTGCAATCAGGTGAATTCGTTTCT-3′. The PCR product was digested with NdeI and XhoI and cloned into the pETDuet-1 vector (Novagen) digested with the same restriction enzymes.

Ty1-IN Purification and Mass Spectrometry—200 ml of Y7092 transformed with pJEF724 (*pGAL1-Ty1-H3*) or empty vector (pRS326) was grown to log phase in SC-Ura + 2% raffinose + 0.1% dextrose at 25 °C. Cells were washed, diluted, and resuspended in 1 liter of SC-Ura + 2% galactose to induce *pGAL1-Ty1-H3* expression for 24 h. Cells were harvested and resuspended in lysis buffer (50 mM Hepes, pH 7.5, 0.1% Nonidet P-40, 150 mM NaCl, 5 mM EDTA, and protease inhibitors) on ice followed by addition of glass beads and lysed. Lysates were centrifuged at 12,000 rpm for 5 min at 4 °C, and supernatant was retained as whole cell protein lysate. 10 μl of anti-IN 8b11 antibody (a kind gift from Jef Boeke (27)) was incubated for 10 min with 360 μl of washed PureProteome Protein G magnetic beads and then washed three times with PBS + 0.1% Tween 20.

The anti-IN-bound beads were split in half, added to 50 mg of protein lysate from each of the *pGAL1-Ty1-H3* and pRS326 harvested cells, and incubated for 2.5 h at 4 °C. The magnetic beads were washed three times with PBS, supernatant was removed, and 45 μl of 1× SDS loading buffer without β-mercaptoethanol was added and placed at 65 °C for 15 min. Beads were spun down, and the supernatant was run on an SDS-polyacrylamide gel. Samples were processed using in-gel digestion (28) in which gel slices corresponding to IgG chains (25 and 55 kDa) were treated separately. Purified peptides were analyzed using an LTQ-Orbitrap Velos (Thermo Fisher Scientific) on line-coupled to an Agilent 1100 Series nanoflow HPLC using a nanospray ionization source (Thermo Fisher Scientific) using the same settings as described previously (29). A 60-min LC gradient (5–35% acetonitrile in 0.5% acetic acid) was used. The LTQ-Orbitrap was set to acquire a full-range scan at 60,000 resolution from 300 to 1,600 thomsons. 10 MS/MS collision-induced dissociation spectra were collected.

Analysis of Mass Spectrometry Data—The spectrum files were processed using MaxQuant (v1.5.1.0) (30–32), and the "label free quantification (LFQ)" and "dependent peptide search" functions were selected. The derived peak list was searched against the reference yeast proteome downloaded from UniProt on June 12, 2012 (6,674 sequences), and the false discovery rate was set to 1%.

GFP and Anti-HA Co-immunoprecipitations (IPs)—GFP and anti-HA IPs were performed as described (23) with the following modifications. For GFP IPs in Figs. 2–4, 1.5 mg of yeast lysate was used, and after Rpc-GFP protein purification, beads were washed three times in wash buffer (50 mM Tris-HCl, pH 7.5, 0.5% Nonidet P-40, and 0.5 mM EDTA) with low salt (300 mM NaCl) or high salt (500 mM NaCl). For GFP IPs in Fig. 9, 2 mg of yeast lysate was used, and beads were washed three times in low salt (300 mM NaCl) wash buffer. For anti-HA IPs (Fig. 2), 2 mg of lysate was mixed with 20 μl of a 1:1 slurry of anti-HA-agarose beads (Covance) for 1.5 h at 4 °C. After washes, the beads were resuspended in 25 μl of 2× SDS loading buffer, and 9 μl of the immunoprecipitate was loaded on an SDS-polyacrylamide gel for immunoblotting analysis.

Purification of Ty1-IN-S from E. coli—The BSC3A Ty1-IN-S expression vector was transformed into BL21(DE3) *E. coli* cells. Transformants were inoculated into 5 ml of LB with ampicillin, grown overnight at 37 °C, then diluted 1:100 in 200 ml, and regrown to an A_{600} of 0.6. Ty1-IN-S expression was induced by adding 1 mM isopropyl 1-thio-β-D-galactopyranoside and growing cells for 1 h at 37 °C. Cells were harvested, resuspended in 20 ml of ice-cold lysis buffer (20 mM Tris-HCl, pH 7.5, 150 mM NaCl, and 0.1% Triton X-100), and lysed by sonication on ice with 35% output amplitude for 3 min (QSonica; 5 s on, 10 s off). The soluble lysate was separated from the cell debris by a 20-min centrifugation at 39,000 × *g* at 4 °C. Ty1-IN-S was purified by adding 400 μl of a 1:1 S-protein-agarose slurry (Novagen) to the lysate and incubating for 1 h at 4 °C followed by washing three times with lysis buffer. The S-protein-agarose with captured Ty1-IN-S was stored at 4 °C and used for the *in vitro* binding assay within 1 week.

Purification of RNA Pol III Proteins—For RNA Pol III purification, *S. cerevisiae* strain NZ16 (33) (originally constructed by Nick Zecherle and Benjamin Hall) containing a hexahistidine tag followed by four tandem FLAG epitope tags at the N terminus of the Rpc128 gene, was grown to an A_{600} of 6 at 30 °C in 200 liters of yeast extract-peptone-dextrose medium. The 200-liter yeast culture was harvested and subsequently lysed by bead beating. The purification scheme was based on the method developed by Cramer and co-workers (34); however, the columns used for tandem chromatography were modified to heparin-Sepharose (GE Healthcare), Talon metal affinity resins (Clontech), DEAE-Sepharose (GE Healthcare), and Mono Q (GE Healthcare). The yield was ~1 mg. Detailed procedures and the chromatography program are available upon request. Recombinant Rpc82, Rpc34, Rpc31, Rpc53, and Rpc37 protein samples were purified as described previously (35, 36). The recombinant Rpc25/17 complex protein sample was purified with a modified purification scheme based on a method described previously (37). The following columns were utilized for tandem chromatography: nickel-Sepharose (GE Healthcare), heparin-Sepharose, and Mono Q.

Ty1-IN-S in Vitro Binding Assay—5 μg of purified RNA Pol III protein was used in each *in vitro* binding assay. 200 μl of lysis buffer was added and incubated with 10 μl of the Ty1-IN-S-agarose slurry (~5-μg eq of Ty1-IN-S protein) for 1 h at 4 °C. 5 μg of purified RNA Pol III protein was added to an equal amount of S-protein-agarose (without Ty1-IN-S bound) for the negative control. The agarose resin was spun down at 5,000 × *g* for 1 min, and the supernatant was collected (unbound fraction). The resin was washed three times with 1 ml of lysis buffer. For the Rpc34 binding assay, the resin was washed an additional three times with lysis buffer containing 300 mM NaCl. Proteins were eluted (bound fraction) by boiling in 20 μl of 2× SDS loading buffer, separated by SDS-PAGE, and detected by immunoblotting. 5 μl of the supernatant was loaded for the unbound fraction, and 5 μl of the bound fraction was loaded. 333 ng of purified protein was loaded to represent 1/15 of the input RNA Pol III protein. A monoclonal antibody against the S-tag (EMD Millipore) was used to detect Ty1-IN-S. A monoclonal antibody against His (HIS.H8, AbLab, University of British Columbia) was used to detect Rpc53-His_6, Rpc37-His_6, Rpc82-V5-His_6, and His_6-MBP-Gal4. A monoclonal antibody against FLAG (Sigma) was used to detect Rpc25/17-FLAG and RNA Pol III with $FLAG_4His_6$-tagged Rpc128. A polyclonal antibody raised against RNA Pol III was used to detect Rpc31 and Rpc34 (38).

SUF16 PCR Assay—The *SNR33* and Ty1 PCR primers and *CPR7* primers have been previously described (39). 1 and 2 μg of yeast genomic DNA were used for the *SUF16* PCR in Figs. 6 and 7, respectively. 5 ng of yeast genomic DNA was used for all *CPR7* PCR assays.

Subtelomere PCR Assay—The following primers were used: OSC66, 5′-CCAAGGATCTAGGTGAGGCTTTGAGAA-3′ (Chr XIV left end 13,634–13,669 bp (*SNZ2*) and Chr VI left end 11,739–11,765 bp (*SNZ3*)); OSC68, 5′-GACATGGGCCCCT-GTTGCTTATATTGT-3′ (Chr IV left end 12,021–12,047 bp (*HXT15*), Chr X right end 733,753–733,779 bp (*HXT16*)); OSC70, 5′-CACAGAGCTTCAGGTTAGGAGCTTCTG-3′ (Chr XV right end 1,072,647–1,072,673 bp (*FDH1*), Chr XVI left end 18,198–18,224 bp (*FDH2*)). 1.5 μg of yeast genomic

DNA was used for the PCR in Fig. 8. 5 ng of yeast genomic DNA was used for the *CPR7* PCR assay in Fig. 8.

Transposition Assays—Ty1 transposition mobility assays were performed as described (23) with the following modifications. For Fig. 6*C* (WT and *rpo31-698*, *rpc34-1*, and *rpc40-V78R* mutants), 2,000 cells were inoculated into 1 ml of SC-Ura medium, and for Fig. 7*C* (*RPC53* and *rpc53Δ11–40*, *rpc53Δ316–350*, and *rpc53Δ2–280* mutants), 200,000 cells were inoculated into 1 ml of SC-Ura-Leu medium. Cells were grown for 5 days at 20 °C, 200 cells were plated for viability (SC-Ura plates for *rpc* mutants and SC-Ura-Leu for *rpc53* mutants), and 10^7 cells were plated for transposition frequency (SC-Ura-His plates for *rpc* mutants and SC-Ura-Leu-His plates for *rpc53* mutants).

Quantitative PCR (qPCR)—Cells were grown in yeast extract-peptone-dextrose medium at 20 °C to logarithmic growth, and 1×10^7 cells were spun down and stored at −80 °C. Total RNA was prepared with a Qiagen RNeasy kit, and 1 μg of RNA was used for cDNA synthesis with a Superscript VILLO cDNA synthesis kit (Invitrogen). Real time PCR was performed in triplicate with 2 μl of diluted cDNA (1:50) and Power SYBR Green Master Mix (Invitrogen). A standard 2-h comparative PCR analysis was performed using a 7500 Real Time PCR System (Applied Biosystems). The primers for the *tLEU*, *tLEU de novo*, and *tGLY* genes have been described (24). qPCR analysis was performed using the comparative C_T method ($\Delta\Delta C_T$ method, Applied Biosystems) with *TAF10* used as an internal control. The *TAF10* primers were: OVM695 5′-GGCGTGCAGCAGATTTCAC-3′ and OVM696 5′-TGAGCCCGTATTCAGCAACA-3′.

The ΔC_T mean value for each sample was calculated by subtracting the C_T mean value for *TAF10* from the C_T mean value of the target (*tLEU*, *tLEU de novo*, or *tGLY*). The $\Delta\Delta C_T$ was calculated by subtracting the ΔC_T mean value of the target gene from each mutant from the value of the target gene from the wild type. The relative quantity (RQ) was calculated as $2^{-\Delta\Delta CT}$ so that the wild type (2^0) is a value of 1.0 and every other value is a relative comparison with wild type. The ΔC_T standard error (S.E.) was both added and subtracted from the $\Delta\Delta C_T$, and the resultant value ($\Delta\Delta C_T$ S.E.) was calculated as $2^{-\Delta\Delta CT\ \text{S.E.}}$ and then subtracted from the $2^{-\Delta\Delta CT}$ value to generate the S.E. error bars for the graphs in Fig. 7, *D–F*.

Results

Ty1-IN Co-purifies with RNA Pol III Subunits—To identify proteins that interact with Ty1-IN and target Ty1 transposon insertion upstream of Pol III-transcribed genes, we purified Ty1-IN from yeast cells. Despite the fact that there are 32 full size Ty1 elements in the S288C genome, Ty1-IN is produced at very low levels. Therefore, we induced expression of Ty1-IN from a *GAL1* promoter-driven Ty1 element, *pGAL1-Ty1-H3*, which induces overexpression of Gag and Pol polypeptides and therefore transposition (Fig. 1*A* and Ref. 40). Ty1-IN was purified using a monoclonal antibody (8b11) after overexpression of *pGAL1-Ty1-H3* and, as a control, from cells carrying vector alone (Fig. 1*A* and Ref. 27). We performed two independent Ty1-IN purifications that were analyzed by label-free quantitative MS analysis. The peak intensity areas for each peptide were measured and summed for a given protein in each of the four samples analyzed (2 × Ty1-IN and control IPs). We then compared the intensities between the Ty1-IN and control purifications and only further considered proteins enriched more than 2-fold. Our MS data confirmed the enrichment of Ty1-IN peptides in the purification from cells with Ty1-IN overexpression *versus* control in both experiments (Table 2). In the second experiment, other Ty1 polypeptides were also enriched to a lower extent, presumably due to purification of a small portion of uncleaved or partially cleaved Ty1. In agreement, we also identified a few peptides spanning two polypeptides (Gag/PR and IN/RT; Table 2). In addition to IN peptides, we also identified 84 and 96 proteins that were enriched more than 2-fold in the Ty1-IN overexpressed purification compared with control in the first and second experiments, respectively (Fig. 1*B*). Of the 12 proteins that were enriched in both experiments, five are RNA Pol III subunits (Rpc25, -34, -40, -53, and -82), whereas Maf1 is a Pol III repressor protein (Fig. 1, *B* and *C*). We also identified Rpc37 and Rpc17 peptides in experiment 1 (Fig. 1*C*). Five Pol III subunits are specific to Pol III: the Rpc53/37 heterodimer, which is the structural counterpart of TFIIF, and the Rpc82/34/31 heterotrimer, which is related to TFIIE in Pol II-mediated transcription (25, 41). We identified four of the five Pol III-specific subunits in our Ty1-IN purifications: Rpc53/37 and Rpc82/34. We also identified the Rpc25/17 subcomplex, which is analogous to Rpb4/7 and Rpa14/43 in Pol II and Pol I, respectively, and Rpc40 (AC40), which is a subunit of both Pol I and Pol III (Fig. 1*C* and Ref. 25).

We validated the physical interaction of Ty1-IN with Pol III subunits by selecting Rpc17,19,37,40,53,82-GFP tagged proteins from the GFP-tagged protein collection and performing a reciprocal IP (42). As described above, Ty1-IN was overproduced using the *pGAL1-Ty1-H3* expression plasmid (40). We purified each Rpc-GFP protein using GFP-Trap beads followed by immunoblotting analysis and probed for the presence of Ty1-IN. We confirmed that Ty1-IN co-purified with Rpc17, -37, -53, and -82 but was not in the immunoprecipitate from the untagged strain after both low salt and high salt washes (Fig. 2*A*). We only detected processed Ty1-IN in the lower molecular weight region of the immunoblot and not in the region where unprocessed PR-IN or IN-RT polypeptides migrate as shown in the α-IN blot of the whole cell lysate (Fig. 2*A*, *left panel*). We detected a faint amount of Ty1-IN in the Rpc40-GFP purification after a low salt wash, but this was removed after a high salt wash (Fig. 2*B*). Next, we tested Rpc19 (AC19), which interacts with AC40 and is also a shared Pol I and Pol III subunit (43, 44). Ty1-IN was able to co-purify with Rpc19-GFP (Fig. 2*B*). Although the Pol III Maf1 repressor was identified in our Ty1-IN MS data, we did not detect an interaction between Ty1-IN and Maf1-GFP or between Ty1-IN and Rpb6, which is part of the central core of Pol III and also shared with Pol I and Pol III (Fig. 2, *A* and *B*).

We were not able to test Rpc25, Rpc31, or Rpc34 using the GFP-Trap system because our attempts to tag these proteins with GFP resulted in cell lethality. Similarly, 3HA and 13Myc epitope tagging was also lethal for Rpc31. However, Rpc34 and Rpc25 were successfully tagged with 3HA, and we performed a co-IP using anti-HA resin with 3HA-tagged cells carrying the

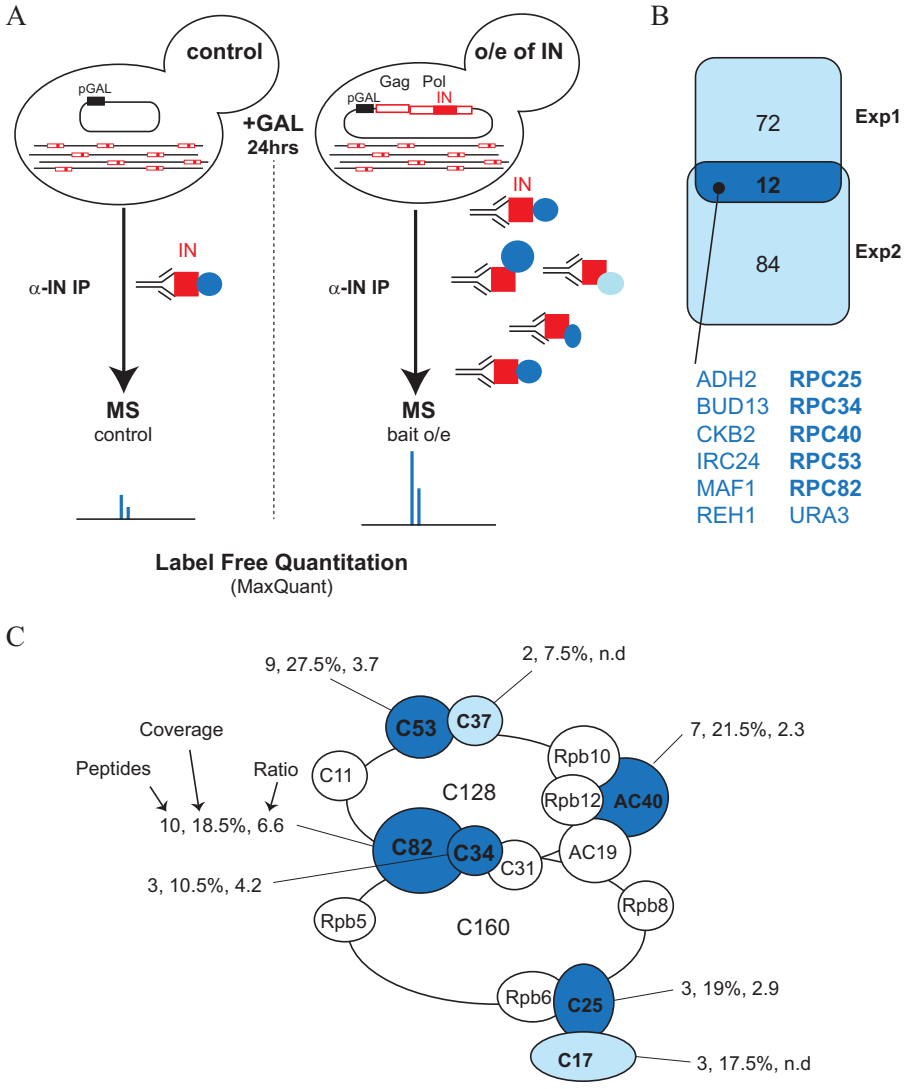

FIGURE 1. **Ty1-IN co-purifies with RNA Pol III subunits.** *A*, schematic of the Ty1-IN purification and MS procedure. Control cells carry a *pGAL1* plasmid vector, whereas Ty1-IN-overexpressing (*o/e of IN*) cells carry the *pGAL1-Ty1-H3* vector (pJEF724) that induces Ty1 element expression upon galactose (+*GAL*) addition (40). After 24 h of galactose treatment, Ty1-IN (*red squares*) was bound to anti-IN antibodies (*horizontal Y shape*), and the co-purified proteins (*blue circles*) were purified using IgG-Sepharose beads (not depicted). Purified proteins were subjected to MS analysis using label-free quantitation. *B*, Venn diagram representing proteins enriched in each and both experiments (experiment 1 (*Exp1*) and experiment 2 (*Exp2*)). *C*, schematic of RNA Pol III adapted from Ref. 46 and colored subunits that were identified in the Ty1-IN MS data. *Dark blue* proteins were identified as Ty1-IN interactors in both experiments 1 and 2, whereas *light blue* proteins were identified in one experiment only. For each Pol III subunit identified by MS, the number of peptides, percent coverage of the protein, and peptide intensity ratios in the IN overexpression IP *versus* the control IP are shown. Only intensity ratios of peptides identified in the two replicates are shown (*n.d.*, not determined).

TABLE 2

Total intensities of Ty peptides in the indicated IPs

Polypeptide	Peptides Exp1	Total intensity (IN IP)	Total intensity (control IP)	Ratio	Peptides Exp2	Total intensity (IN IP)	Total intensity (control IP)	Ratio
Gag	9	4.35×10^9	2.42×10^9	1.8	11	1.45×10^{10}	3.41×10^9	4.3
PR	3	1.15×10^8	8.84×10^7	1.3	1	3.33×10^8	8.78×10^7	3.8
IN	10	3.4×10^9	7.56×10^8	4.5	11	1.95×10^9	1.47×10^8	13.3
RT	3	8.64×10^8	8.55×10^8	1	4	2.06×10^8	6.87×10^7	3

pGAL1-Ty1-H3 expression plasmid (Fig. 2*C*). Both Rpc34-3HA and Rpc25-3HA were able to interact with Ty1-IN after a low salt wash, but the interaction was minimal after a high salt wash (Fig. 2*C*). As seen with the GFP system, Rpc82-3HA interacted with Ty1-IN after both a low and high salt wash (Fig. 2*C*).

Our co-IP interaction data indicate that Ty1-IN interacts with multiple RNA Pol III proteins, including the RNA Pol III-specific Rpc82/34/31 and Rpc53/37 subcomplexes (Fig. 2, *A–C*). A weaker interaction, or no interaction, is detected with some of the shared RNA Pol components such as Rpc40 (Pols I and III) and Rpb6 (Pols I, II, and III), respectively, although Rpc19 (Pols I and III) interacts well with Ty1-IN (Fig. 2*B*).

Ty1-IN Does Not Interact with RNA Pol II, TFIIIB, or TFIIIC—RNA Pol III is a stable complex and requires partially denaturing conditions to remove subcomplexes; therefore it is likely that when individual subunits are purified the remainder

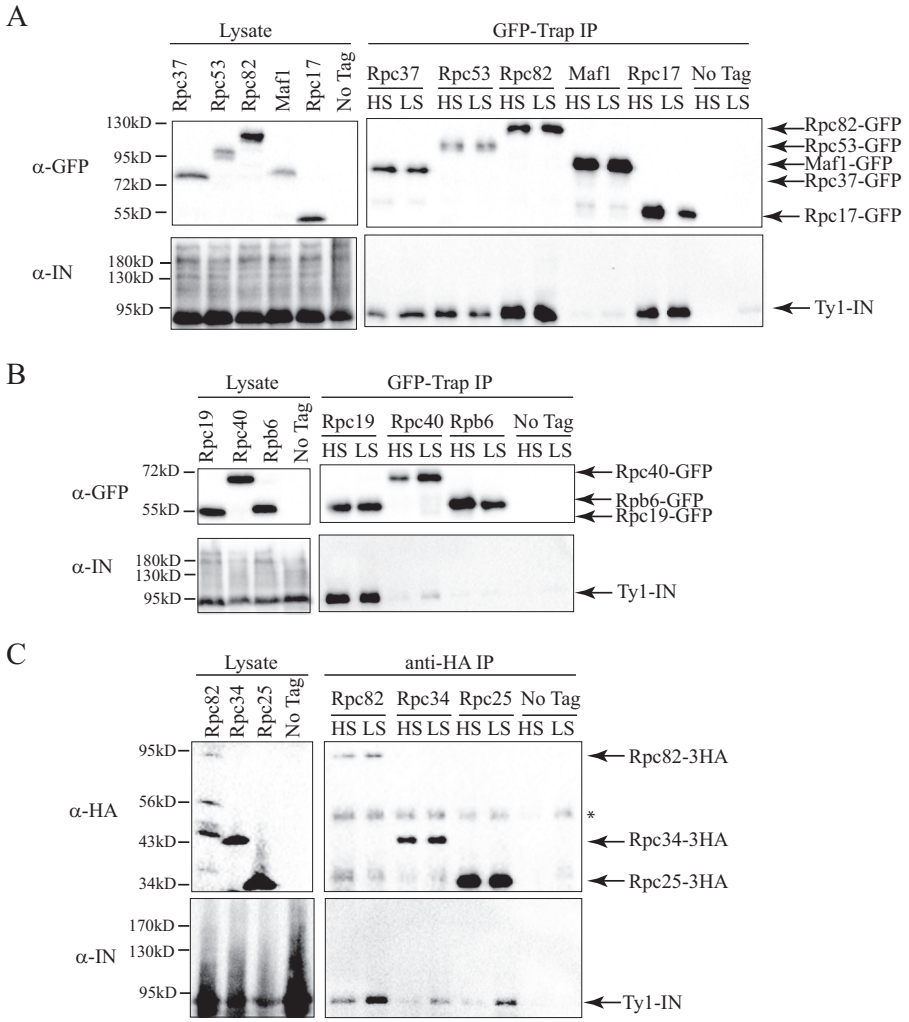

FIGURE 2. **Ty1-IN interacts with RNA Pol III subunits.** *A*, immunoblot of whole cell lysate (*Lysate*) and GFP-Trap IP carried out from Rpc37-GFP, Rpc53-GFP, Rpc82-GFP, Maf1-GFP, Rpc17-GFP, and untagged wild type (*No Tag*) cells. *B*, immunoblot of whole cell lysate (*Lysate*) and GFP-Trap IP carried out from Rpc19-GFP, Rpc40-GFP, Rpb6-GFP, and untagged wild type (*No Tag*) cells. *C*, immunoblot of whole cell lysate (*Lysate*) and anti-HA IP performed from Rpc82-3HA, Rpc34-3HA, Rpc25-3HA, and untagged wild type (*No Tag*) cells. The *asterisk* marks the heavy chain antibody. For *A–C*, expression of a Ty1 element (*pGAL1-Ty1-H3*, pJEF724) was induced in all strains for 24 h prior to cell lysis. Immunoprecipitates were washed with either a high salt (*HS*; 500 mM NaCl) or low salt (*LS*; 300 mM NaCl) wash. Immunoblots were probed with anti-GFP (*A* and *B*), anti-HA (*C*), and anti-IN (8b11) (*A–C*) antibodies.

of the Pol III complex is co-purified (45, 46). To test whether Ty1-IN also interacts with the two largest core RNA Pol III subunits, we purified Rpc160-GFP and Rpc128-GFP and demonstrated that indeed Ty1-IN is present in the purification (Fig. 3*A*). Because Ty1 elements insert within a ~1-kbp window upstream of tRNA genes, there remained the possibility that Ty1-IN could also interact with RNA Pol II. However, we found no evidence of interaction between Ty1-IN and the counterparts of Rpc160 and Rpc128, Rpb1 and Rpb2, respectively (Fig. 3*A*).

Because Ty1 element insertion requires active Pol III transcription, we were curious whether other factors required for Pol III transcription may associate with Ty1-IN. To activate tRNA transcription, TFIIIC recognizes and binds to tRNA promoters followed by TFIIIB assembly and recruitment of the RNA Pol III complex (47). An interaction between Ty3-IN and the TFIIIB factor Brf1 is sufficient to target the Ty3 element to Pol III transcription start sites *in vitro* (6–8). We tested whether a subset of the TFIIIB (Brf1 and Bdp1) and TFIIIC (Tfc1, -3, and -7) subunits co-purify with Ty1-IN using the GFP tag system. However, we were unable to detect any interaction between Ty1-IN and TFIIIB or TFIIIC subunits (Fig. 3, *B* and *C*). Therefore the mechanism of Ty1-IN and Ty3-IN interaction with the Pol III transcription apparatus is different.

RNA Pol III Interacts with the C Terminus of Ty1-IN—The domain structure of Ty1-IN is similar to other retroviral integrases and contains an N-terminal HHCC zinc-binding domain, a catalytic core domain, and a less conserved C-terminal domain (Fig. 4*A* and Ref. 48). A bipartite nuclear localization signal (NLS) resides at the end of Ty1-IN with two basic regions (NLS1 and NLS2) separated by 21 amino acids (Fig. 4*D* and Refs. 49 and 50). We used previously generated Ty1-IN deletion constructs to map the domain of Ty1-IN that interacts with RNA Pol III (Fig. 4*A* and Ref. 49). Co-IP analysis was performed by GFP-Trap purification of Rpc82-GFP in a strain expressing either full-length Ty1-IN or a Ty1-IN deletion construct. Rpc82-GFP interacted with full-length Ty1-IN, Ty1-IN with amino acids 422–515 removed (IN-C), or Ty1-IN with

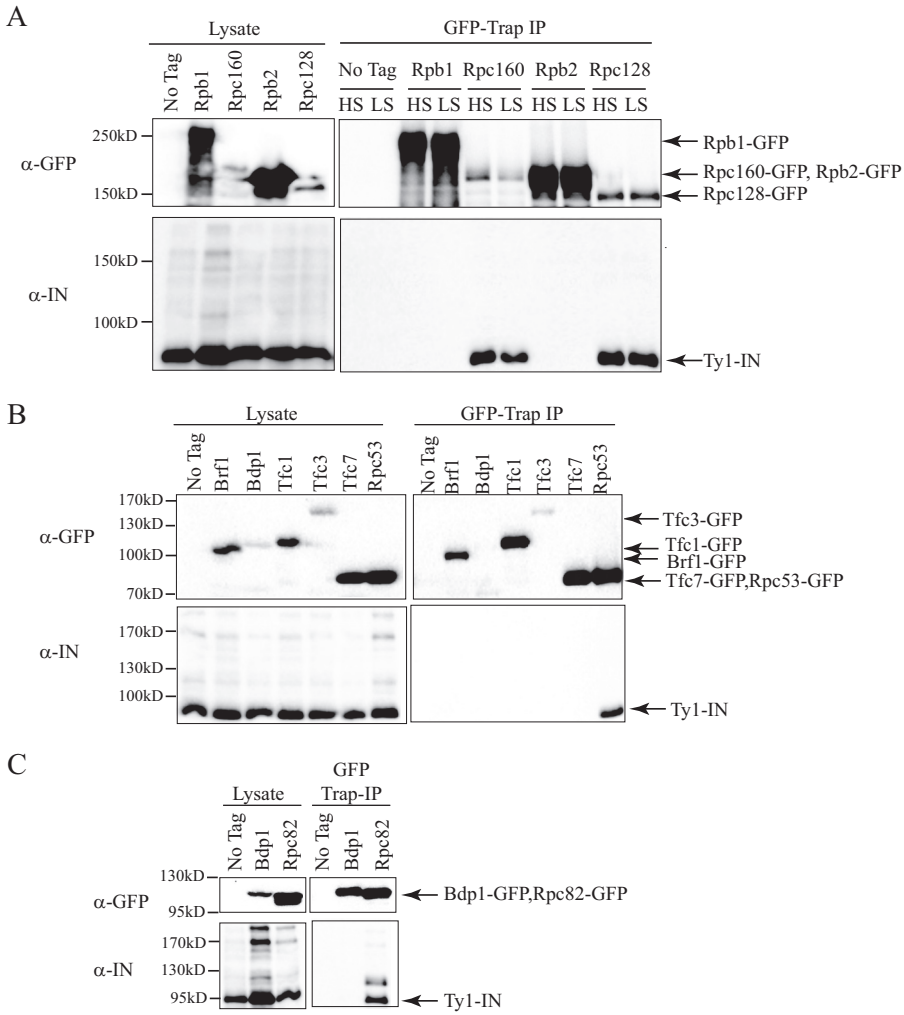

FIGURE 3. **Ty1-IN interacts with Rpc160 and Rpc128 Pol III core subunits but not Pol II, TFIIIB, or TFIIIC subunits.** *A*, immunoblot of whole cell lysate (*Lysate*) and GFP-Trap IP performed from untagged wild type (*No Tag*), Rpb1-GFP, Rpc160-GFP, Rpb2-GFP, and Rpc128-GFP cells. *B*, immunoblot of whole cell lysate (*Lysate*) and GFP-Trap IP performed from untagged wild type (*No Tag*), Brf1-GFP, Bdp1-GFP, Tfc1-GFP, Tfc3-GFP, Tfc7-GFP, and Rpc53-GFP cells. *C*, immunoblot of whole cell lysate (*Lysate*) and GFP-Trap IP performed from untagged wild type (*No Tag*), Bdp1-GFP, and Rpc82-GFP cells. For *B*, 1 mg of lysate was used per immunoprecipitate. For *C*, 3 mg of lysate was used for the GFP-Trap IP from the untagged and Bdp1-GFP strains, whereas 1.5 mg was used for the GFP-Trap IP from the Rpc82-GFP strain. For *A–C*, expression of a Ty1 element (*pGAL1-Ty1-H3*, pJEF724) was induced in all strains for 24 h prior to cell lysis. Blots were probed with anti-GFP and anti-IN (8b11) antibodies. *HS*, high salt (500 mM); *LS*, low salt (300 mM).

amino acids 515–561 removed (IN-F) but not any construct with the C-terminal amino acids 561–635 removed (IN-D, IN-E, and IN-G; Fig. 4*A*). As well, the N-terminal 422 amino acids of Ty1 were not able to interact with Rpc82-GFP (IN-A; Fig. 4*A*). None of the Ty1-IN fusion proteins interacted with the GFP-Trap beads in the absence of Rpc82-GFP (Fig. 4*B*). We also tested whether Rpc82-GFP could interact with Ty1-IN carrying mutations in basic region 1 (NLS1) or both basic regions (IN-NLS1+2) of the NLS (Fig. 4*D* and Ref. 49). Mutation of the Ty1-IN NLS1 and NLS2 regions completely abrogated the interaction with Rpc82 (Fig. 4*D*). Because the cell lysis procedure disrupts the nuclear and cytoplasmic compartments, we do not think the lack of interaction is due to IN-NLS1+2 being excluded from the nucleus, although we cannot entirely rule out this possibility. However, when combined with the Ty1-IN truncation analysis, our data suggest that the C-terminal 75 amino acids of Ty1-IN interact with RNA Pol III, which concurs with a recent studying showing a two-hybrid interaction between Rpc40 and Ty1-IN that was abrogated by removal of the C-terminal amino acids 578–635 (24). Although Bridier-Nahmias *et al.* (24) found that Ty1-IN amino acids 578–635 were also sufficient to interact with Rpc40 using a two-hybrid assay, we were unable to detect an interaction of a C-terminal Ty1-IN fragment (amino acids 422–636; IN-B) with Rpc82 or Rpc53 by co-IP (Fig. 4*C*). Possibly there is an inhibitory domain in Ty1-IN amino acids 422–578, or the requirements for Ty1-IN interaction with different RNA Pol III subunits have subtle differences.

RNA Pol III Interacts with Ty1-IN in Vitro—Our co-IP analysis demonstrates that Ty1-IN interacts with multiple RNA Pol III proteins when purified from yeast extracts (Fig. 2). However, due to the stability of the RNA Pol III complex, the entire complex is likely purified in each IP, and therefore the Pol III protein(s) that interacts directly with Ty1-IN cannot be determined by this method. To determine which RNA Pol III proteins Ty1-IN may interact with directly, we used an *in vitro* approach. Ty1-IN containing a C-terminal S-tag was expressed and purified from *E. coli* with S-protein-agarose and mixed

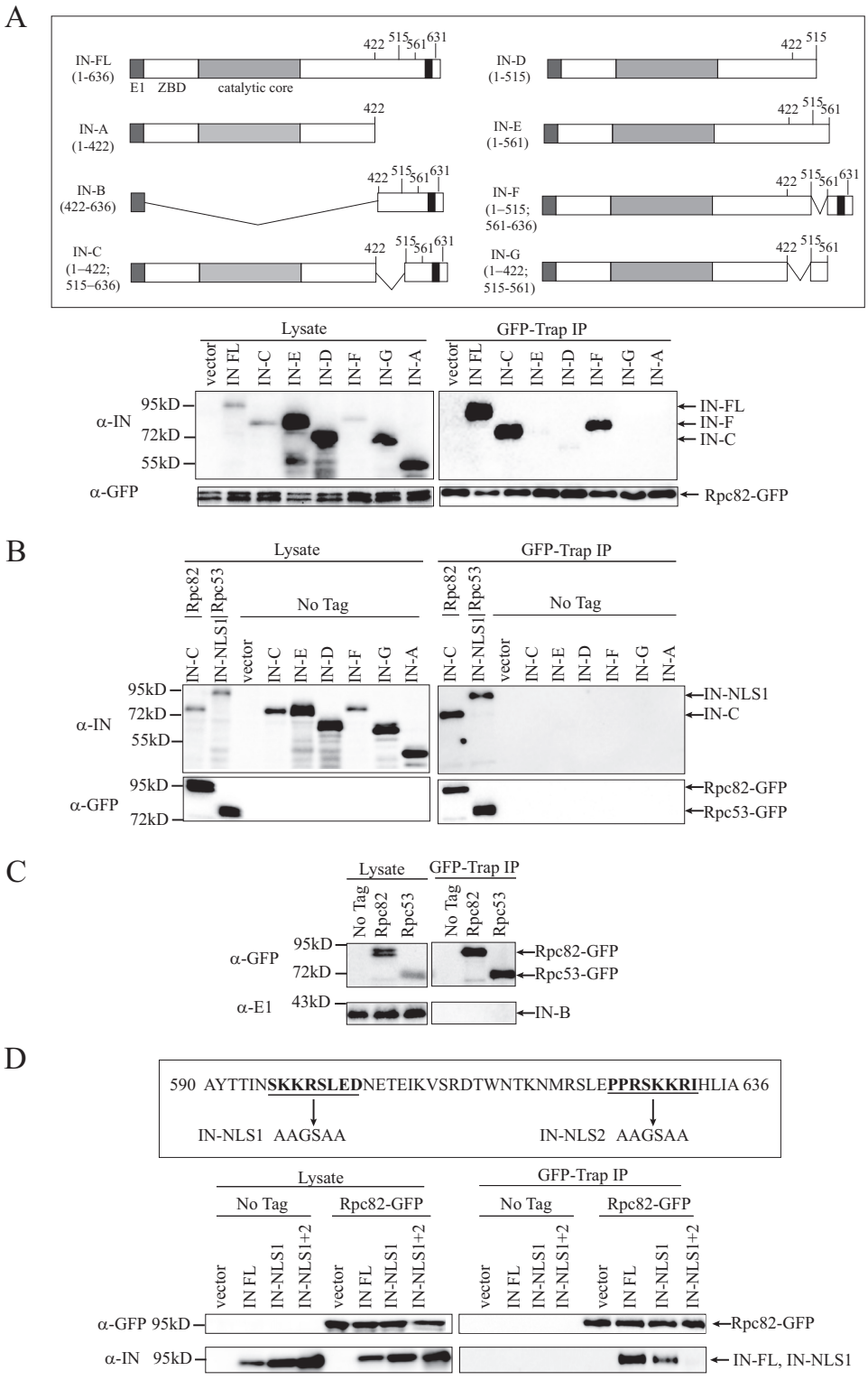

FIGURE 4. **Rpc82 interacts with the C terminus of Ty1-IN.** *A*, *upper panel*, schematic of E1 epitope-tagged Ty1-IN fusion proteins as described (49). E1 tag is *dark gray*, zinc binding domain (*ZBD*) is *white*, the IN catalytic core is *light gray*, and the NLS is *black*. *Numbers* shown represent amino acids. *Lower panel*, immunoblot of whole cell lysate (*Lysate*) and GFP-Trap IP performed from Rpc82-GFP-tagged cells carrying the indicated vector alone, E1-tagged full-length Ty1-IN fusion (*IN-FL*), or E1-tagged fusions to the indicated Ty1-IN truncations. To the *right* of the panel, the IN fusions that interact with Rpc82-GFP are shown. *B*, immunoblot of whole cell lysate (*Lysate*) and GFP-Trap IP performed from Rpc82-GFP cells carrying the IN-C fusion, Rpc53-GFP cells carrying the IN-NLS1 fusion, and untagged (*No Tag*) cells carrying vector alone and the indicated Ty1-IN fusions. *C*, immunoblot of whole cell lysate (*Lysate*) and GFP-Trap IP performed from untagged (*No Tag*), Rpc82-GFP-, or Rpc53-GFP-tagged cells carrying the C-terminal 422–636 amino acids of IN fused to E1 (*IN-B*). *D*, *upper panel*, location of the IN-NLS1 and IN-NLS2 mutations at the C terminus of Ty1-IN (amino acids 590–636 as described (49)). The mutated amino acid residues are in *bold* and *underlined*, and the *arrow* points to the mutated amino acid sequence. *Lower panel*, immunoblot of whole cell lysate (*Lysate*) and GFP-Trap IP performed from Rpc82-GFP-tagged cells carrying vector or the E1-tagged IN-FL, IN-NLS1 mutant, or IN-NLS1+2 mutant. For *A–D*, expression of Ty1-IN fusion proteins was induced for 8 h. For *A*, *B*, and *D*, blots were probed with anti-GFP and anti-IN (8b11) antibodies. For *C*, the blot was probed with anti-E1 and anti-GFP antibodies.

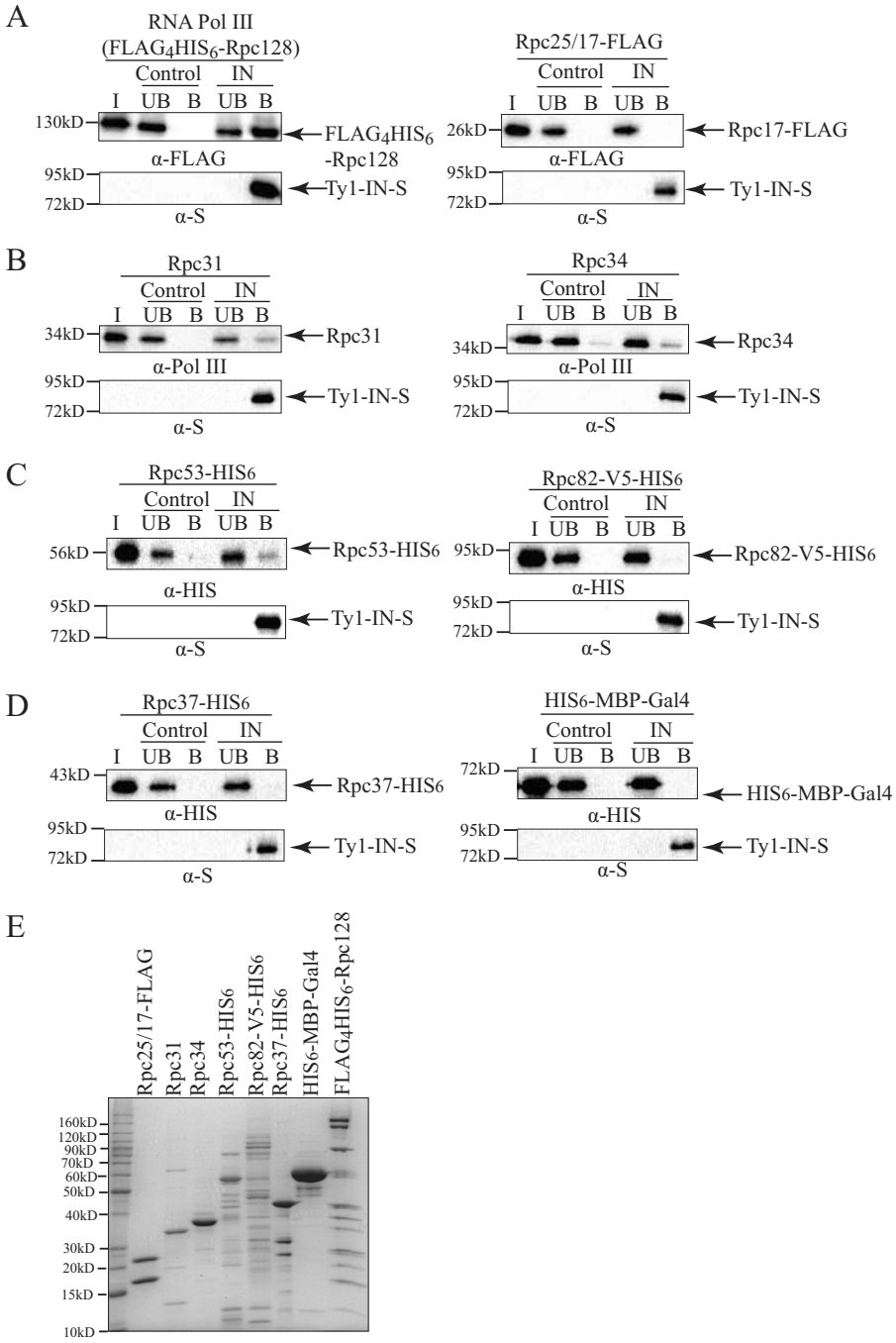

FIGURE 5. **Ty1-IN interacts with RNA Pol III *in vitro*.** *A–D*, Ty1-IN fused to a C-terminal S-tag (Ty1-IN-S) was bound to S-protein-agarose beads and incubated with purified RNA Pol III proteins as described under "Experimental Procedures." The purified RNA Pol III protein is indicated above each immunoblot. For all immunoblots, Ty1-IN-S was visualized with an anti-S (α-*S*) antibody. "*Control*" is S-protein-agarose alone; "*IN*" is Ty1-IN-S bound to S-protein-agarose. The amounts of input protein (*I*), unbound fraction (*UB*), and bound fraction (*B*) loaded on each gel are described under "Experimental Procedures." For *A*, *left panel*, the entire RNA Pol III complex is co-purified with N-terminal $FLAG_4His_6$-tagged Rpc128. For *A*, *right panel*, *Rpc25/17-FLAG* is Rpc17-FLAG co-purified with Rpc25. $FLAG_4His_6$-Rpc128 and Rpc17-FLAG are visualized with anti-FLAG (α-*FLAG*) antibody. *B*, Rpc31 and Rpc34 are purified without epitope tags and are visualized with anti-Pol III antibody (38). *C–D*, Rpc53-His_6, Rpc82-V5-His_6, Rpc37-His_6, and His_6-MBP-Gal4 are all visualized with an anti-His (α-*HIS*) antibody. *E*, Coomassie-stained gel of purified proteins used for *in vitro* assays in *A–D*. 5 μg of each purified protein was loaded except for $FLAG_4His_6$-Rpc128-tagged Pol III for which 20 μg was loaded. All proteins were purified from *E. coli* except Pol III (*A*, *left panel*), which was purified from yeast as described under "Experimental Procedures."

with a $FLAG_4His_6$-Rpc128-tagged RNA Pol III complex purified from *S. cerevisiae* (Fig. 5, *A* (*left panel*) and *E*). S-protein-agarose with no Ty1-IN bound was used as a control. The bound and unbound fractions from the Ty1-IN-S beads and the S beads alone were analyzed by immunoblotting along with the input Pol III protein and probed for the presence of $FLAG_4His_6$-Rpc128. The RNA Pol III complex specifically interacted with the Ty1-IN-S beads but not the S beads alone (Fig. 5*A*). Next, RNA Pol III-specific subunits were purified from *E. coli* and tested individually for interaction with Ty1-IN-S. We were unable to detect an interaction between Rpc25/17-FLAG and Ty1-IN, which also served as a negative control

for the FLAG tag binding to the S beads (Fig. 5, *A* (*right panel*) and *E*). Rpc31 and Rpc34 were both purified without epitope tags and were therefore visualized with antibody raised against the entire Pol III complex (38). Both Rpc31 and Rpc34 were identified in the bound fraction of the Ty1-IN-S beads; albeit some background binding of Rpc34 to the S beads alone was detected (Fig. 5, *B* and *E*). Rpc31 and Rpc34 interact with Rpc82 to form the Rpc82/34/31 Pol III-specific subcomplex; therefore it was of interest to test whether Rpc82 could interact directly with Ty1-IN. Rpc82 was C-terminally fused to a V5-His_6 tag and expressed in *E. coli* as described (35); however, the yield was low as most of Rpc82-V5-His_6 was insoluble. This could be because proper folding of Rpc82 requires a post-translational modification, and Rpc82 is known to be sumoylated in yeast (51). Nevertheless, we tested whether our preparation of Rpc82-V5-His_6 was able to interact with Ty1-IN but failed to detect an interaction with Rpc82 and Ty1-IN-S based on immunoblotting analysis (Fig. 5, *C* (*right panel*) and *E*). Finally, we tested whether the Rpc53 or Rpc37 Pol III-specific proteins could interact directly with Ty1-IN. We found that purified Rpc53-His_6 interacted with Ty1-IN-S beads but not S beads alone (Fig. 5, *C* (*left panel*) and *E*). However, neither purified Rpc37-His_6 nor the His_6-MBP-Gal4 protein (control for His_6 tag) were able to interact with Ty1-IN-S (Fig. 5, *D* and *E*). In summary, we found that a subset of RNA Pol III proteins (Rpc31, Rpc34, and Rpc53) purified from *E. coli* and the purified Pol III complex from yeast are able to interact with Ty1-IN *in vitro*.

rpc34 and rpc40 Temperature-sensitive (ts) Mutants Have Defects in Ty1 Insertion Upstream of the SUF16 tRNA Gene and in Genome-wide Ty1 Mobility—Our *in vivo* co-IP and *in vitro* binding studies suggest that Ty1-IN may interact with multiple RNA Pol III subunits. RNA Pol III ts mutants that were available in a published ts collection (52) were tested for Ty1 element insertion upstream of the *SUF16* tRNA gene, which is a hot spot for Ty1 transposition (53). Although the ts mutants are lethal at high temperatures, Ty1 transposition is induced by growing cells at 20 °C at which temperature the ts mutants are viable. *De novo* Ty1 element transposition upstream of *SUF16* was detected using an established PCR assay with the indicated primers, and the *spt3*Δ mutant is a control that lacks Ty1 element expression (Fig. 6*A* and Ref. 39). We found that all three RNA Pol III mutants (*rpo31-698*, *rpc34-1*, and *rpc40-V78R*) displayed defects in the typical periodic Ty1 element insertion pattern typical of wild type strains (Fig. 6*B* and Ref. 39). The *rpo31-698* RNA Pol III mutant, which carries a mutation in the largest Pol III subunit (Rpc160), had the most similar insertion pattern to wild type, although the levels of insertion were reduced to 37% of wild type (Fig. 6*B*). Both *rpc34-1* and *rpc40-V78R* had highly reduced Ty1 insertion at the *SUF16* locus (10 and 9%, respectively, of wild type). We used a qPCR assay to demonstrate that the ts mutants have similar levels of tRNA gene transcripts to wild type cells; therefore the lack of Ty1 element insertion at *SUF16* is not due to Pol III transcription defects (Fig. 6, *D–F*). Because the *SUF16* tRNA assay analyzes Ty1 insertions at a single locus, we also performed a quantitative assay for Ty1 mobility to examine *de novo* Ty1 insertions in the whole genome. We used a plasmid (pBDG922) that carries

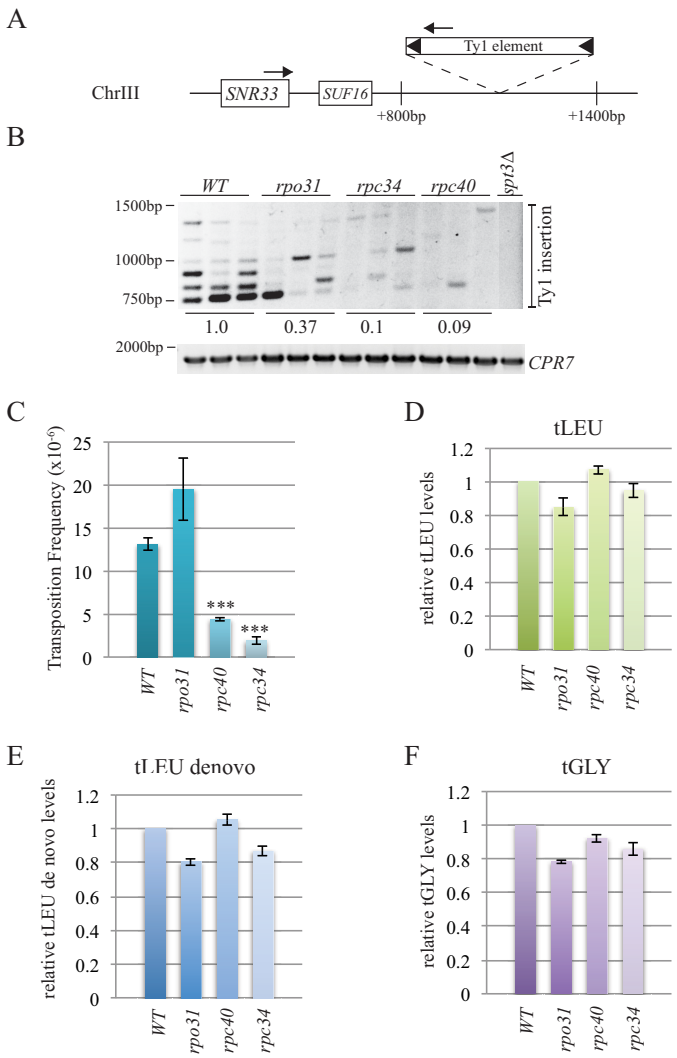

FIGURE 6. **rpc34 and rpc40 mutants have decreased Ty1 element insertion at the *SUF16* locus and reduced Ty1 mobility.** *A*, schematic of the *SUF16* genomic locus with PCR primers (*arrows*) designed to hybridize within the *SNR33* gene and the newly inserted Ty1 elements. *B*, *SUF16* PCR analysis of yeast genomic DNA extracted from wild type (*WT*), *rpo31-698* (*rpo31*), *rpc34-1* (*rpc34*), and *rpc40-V78R* (*rpc40*) strains grown in triplicate and *spt3*Δ (single isolate) at 20 °C for 3 days to induce transposition. The *upper panel* is the result of the PCR assay with primers shown in *A*; the *lower panel* is a control PCR for the *CPR7* locus to demonstrate that yeast genomic DNA was present in each sample. Quantification of Ty1 insertion events is shown relative to wild type. *C*, quantification of Ty1 mobility in WT, *rpo31-698*, *rpc40-V78R*, and *rpc34-1* mutants induced to transpose for 5 days at 20 °C. A minimum of five transformants were quantified per strain. *** represents a significant difference from wild type ($p < 0.001$). *D–F*, qPCR analysis of *tLEU*, *tLEU de novo*, and *tGLY* gene expression in WT, *rpo31-698*, *rpc40-V78R*, and *rpc34-1* mutant strains. The RQ of wild type is set to a value of 1.0, and the mutant RQ values are compared with wild type. *Error bars* are S.E. and were calculated as described under "Experimental Procedures."

a Ty1 element containing the *HIS3* gene with an artificial intron (AI) that interrupts *HIS3* expression (*HIS3AI*). The AI intron is removed after Ty1 expression, and the cell becomes *HIS3*+ after Ty1 cDNA insertion into DNA, which can be quantitated (54). Wild type cells underwent Ty1 transposition at a frequency of 13.1×10^{-6} compared with 4.4×10^{-6} for *rpc40-V78R* and 1.9×10^{-6} for *rpc34-1* (~3- and 7-fold, respectively, less than wild type; $p < 0.0001$). Despite the reduction in Ty1 insertion at the *SUF16* tRNA locus, *rpo31-698* mutant cells did

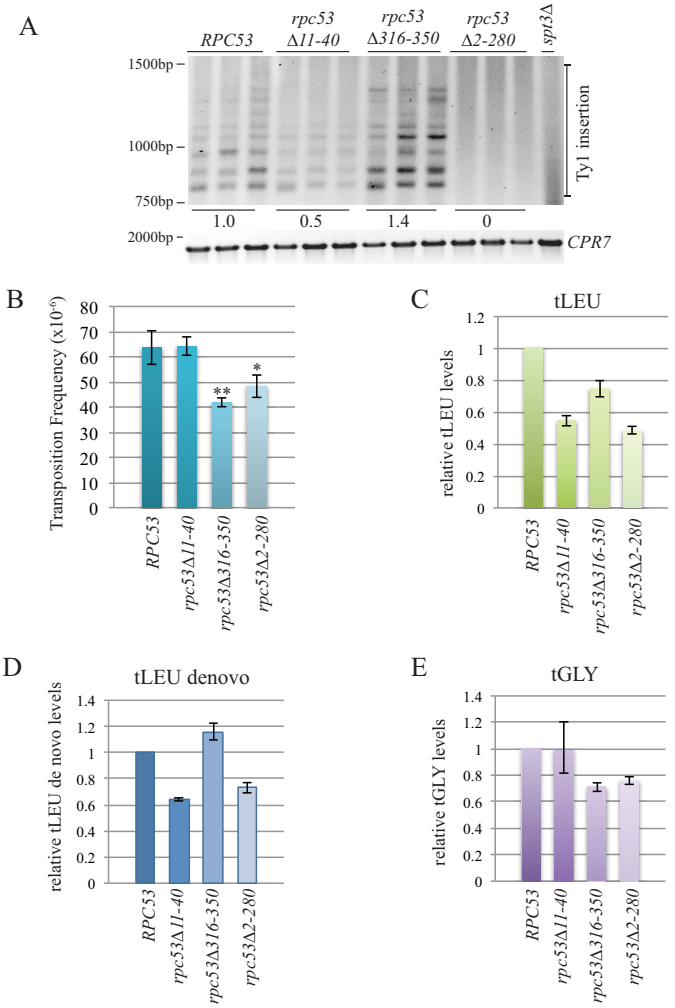

FIGURE 7. **The N terminus of Rpc53 is necessary for Ty1 element insertion upstream of the *SUF16* tRNA gene.** *A*, *upper panel*, *SUF16* PCR analysis of yeast genomic DNA extracted from the indicated strains grown in triplicate for 3 days at 20 °C to induce transposition. *Lower panel*, control PCR for the *CPR7* locus to demonstrate that yeast genomic DNA was present in each sample. Quantification of Ty1 insertion events is shown relative to wild type. *B*, transposition frequency of wild type (*RPC53*) and *rpc53* mutants (*rpc53Δ11–40*, *rpc53Δ316–350*, and *rpc53Δ2–280*) strains induced to transpose for 5 days at 20 °C. A minimum of eight transformants were quantified per strain. * and ** represent significant difference from wild type ($p < 0.1$ and $p < 0.01$, respectively). *C–E*, qPCR analysis of *tLEU*, *tLEU de novo*, and *tGLY* gene expression in wild type (*RPC53*) and *rpc53* mutant (*rpc53Δ11–40*, *rpc53Δ316–350*, and *rpc53Δ2–280*) strains. The RQ of wild type is set to a value of 1.0, and the mutant RQ values are compared with wild type. *Error bars* are S.E. and were calculated as described under "Experimental Procedures."

not have a statistically significant change in Ty1 mobility compared with wild type cells (Fig. 6*C*).

The N Terminus of Rpc53 Is Required for Ty1 Insertion Upstream of the SUF16 tRNA Gene—We analyzed a panel of viable *RPC53* deletion mutants for Ty1 element insertion upstream of the *SUF16* tRNA locus (36). Although an Rpc53 C-terminal mutant (*rpc53Δ316–350*) had slightly increased (~1.4-fold) Ty1 insertion, an N-terminal Rpc53 deletion mutant, *rpc53Δ11–40*, had a 50% reduction in Ty1 insertion, and a larger N-terminal deletion mutant (*rpc53Δ2–280*) was completely deficient in Ty1 element insertion (Fig. 7*A*). We tested tRNA gene expression in *rpc53Δ2–280* cells and found that *tLEU* and *tGLY* transcripts were 48 and 76%, respectively, of wild type values, whereas *tLEU de novo* (*tLEU* transcript prior to splicing) was 73% of wild type (Fig. 7, *C–E*). Although there is a decrease in tRNA gene expression in *rpc53Δ2–280* cells, it is not sufficient to explain a complete lack of Ty1 element insertion upstream of the *SUF16* tRNA gene. However the 50% reduction of *SUF16* Ty1 element insertion in *rpc53Δ11–40* mutant cells could be attributed to defects in tRNA gene transcription, which was reduced to 55% for *tLEU* and 64% for *tLEU de novo* transcripts but at wild type levels for *tGLY* transcripts (Fig. 7, *C* and *D*). Despite the fact that no Ty1 element insertion was detected upstream of the *SUF16* locus in *rpc53Δ2–280* cells, overall Ty1 mobility was reduced to only ~75% of wild type with a frequency of 48.2×10^{-6} compared with 63.7×10^{-6} for wild type cells (Fig. 7*B*). Even though the *rpc53Δ11–40* mutant had reduced Ty1 element insertion at the *SUF16* locus, the overall Ty1 mobility was equivalent to wild type cells (Fig. 7*B*). Finally, the *rpc53Δ316–350* mutant, which had an ~1.4-fold increase in Ty1 element insertion at the *SUF16* locus, had the most reduced overall Ty1 mobility with a frequency of 41.9×10^{-6}, or 65% of wild type. The moderate changes we detected in genome-wide Ty1 insertion frequency in the *rpc53* mutants compared with the 50% reduction in the *rpc53Δ11–40* mutant, and the complete lack of insertion in the *rpc53Δ2–280* mutant at the *SUF16* locus could be because Pol III transcription is differentially affected at different tRNA genes or because the Ty1 element is being targeted elsewhere in the genome.

Ty1 Insertion Is Not Redirected to Chromosome Ends in the rpc53Δ2–280 Mutant—Replacing *S. cerevisiae* Rpc40 with *S. pombe* Rpc40 resulted in retargeting of Ty1 elements to telomere-proximal regions at the ends of chromosomes (24). We tested whether Ty1 elements were being similarly mistargeted in our *rpc53Δ2–280* mutant by designing primers that hybridized to the chromosome ends identified in the Bridier-Nahmias *et al.* (24) study as preferred Ty1 integration sites. Each insertion site is within a gene that has an almost identical homologue (*e.g. SNZ2*/*SNZ3*); therefore each set of primers (one within the Ty1 element and the other within a gene) simultaneously amplified Ty1 elements at two telomere-proximal genomic locations (*e.g.* Chr VI and Chr XIV left end; Fig. 8*A*). The *S. pombe RPC40* and *rpc53Δ2–280* mutant strains and their wild type counterparts were grown for 3 days at 20 °C, and genomic DNA was extracted. It was evident that Ty1 elements were highly amplified from Chr IV, VI, XIV, and XVI left telomere- and Chr X and XV right telomere-proximal regions in the *S. pombe RPC40* strain but not in the *S. cerevisiae RPC40* wild type strain (Fig. 8). We did not find any evidence of hyperamplification of Ty1 elements from these same regions in the *rpc53Δ2–280* mutant or the isogenic wild type strain (Fig. 8). Therefore Ty1 element insertion is not redirected toward chromosome ends in the *rpc53Δ2–280* mutant.

Ty1-IN Interaction with Rpc37 Is Disrupted in rpc53Δ2-280—The lack of Ty1 element targeting upstream of *SUF16* in the *rpc53Δ2–280* mutant suggests that the interaction between Ty1-IN and either the entire Pol III complex or a specific Pol III subunit has been abrogated. We asked whether the interaction between Ty1-IN; the Rpc82/34/31, Rpc53/37, and Rpc17/25 subcomplexes; and Pol III core in

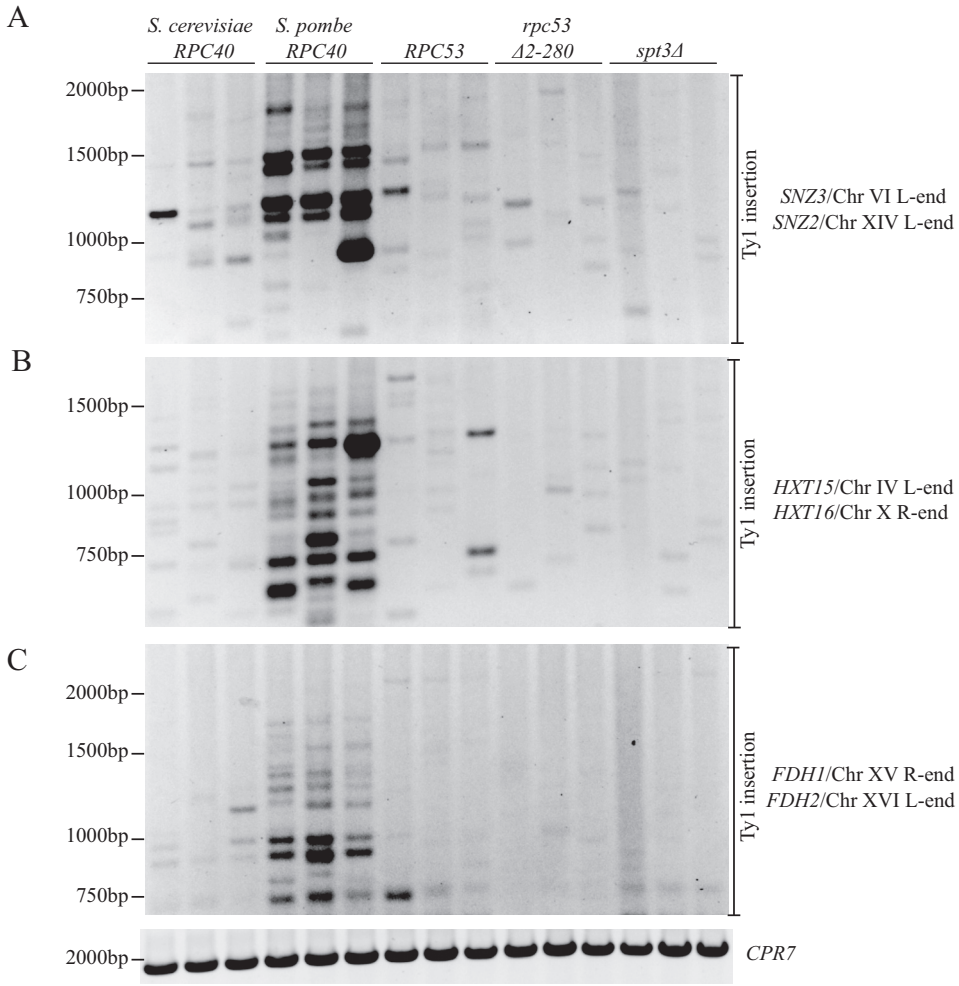

FIGURE 8. **Ty1 insertion is not redirected to telomere-proximal regions in the *rpc53Δ2–280* mutant.** PCR analysis of yeast genomic DNA extracted from the indicated strains grown in triplicate for 3 days at 20 °C is shown. Each PCR contained a Ty1 element primer and a telomere-proximal primer. The telomere-proximal primers hybridize to two genomic regions due to identical DNA sequences at the following loci: *SNZ3*/*SNZ2* (*A*), *HXT15*/*HXT16* (*B*), and *FDH1*/*FDH2* (C). *CPR7* PCR is shown as a control to demonstrate that equal genomic DNA is present in each sample. *R*, right; *L*, left.

the *rpc53*Δ*2–280* mutant was affected by GFP-Trap pull-down of representative GFP-tagged proteins from each complex (Fig. 9). The Pol III core (Rpc19-GFP), Rpc82/34/31 (Rpc82-GFP), and Rpc17/25 (Rpc17-GFP) subcomplexes were all able to interact with Ty1-IN in the *rpc53*Δ*2–280* mutant; however, the Rpc53/37 subcomplex was not (Rpc37-GFP; Fig. 9). Therefore, insertion of Ty1 elements upstream of *SUF16* requires the interaction of Rpc37 and probably also Rpc53 with Ty1-IN.

Discussion

We discovered that Ty1-IN co-purifies from yeast cells with multiple RNA Pol III subunits using MS analysis and validated the interaction by performing co-IPs from yeast lysates (Figs. 1 and 2). Ty1-IN interacts with the two largest Pol III core subunits, Rpc160 and Rpc128, but not the RNA Pol II homologues, Rpb1 and Rpb2, respectively, suggesting that the interaction is specific to RNA Pol III (Fig. 3*A*). The interaction between Ty1-IN and RNA Pol III requires the C terminus of Ty1-IN, but we did not find that the Ty1-IN C terminus alone co-purified with Rpc82 or Rpc53 (Fig. 4). Whether or not the Ty1-IN C terminus is sufficient to interact with RNA Pol III may depend on the subunit tested and the experimental method used. Using the yeast two-hybrid system, the C-terminal 578–635 amino acids of Ty1-IN were sufficient to interact with Rpc40; however, this system cannot exclude that binding is mediated via another protein (24). We performed *in vitro* binding assays to demonstrate that *E. coli*-produced Ty1-IN interacts with RNA Pol III purified from yeast as well as the Pol III-specific proteins Rpc31, Rpc34, and Rpc53 purified from *E. coli* (Fig. 5). The *rpc34-1* and *rpc40-V78R* mutant strains have defects in Ty1 element insertion upstream of the *SUF16* tRNA hot spot locus and in genome-wide transposition frequency (Fig. 6). Interestingly, a strain carrying only the C-terminal third of Rpc53 (*rpc53*Δ*2–280*) is incapable of Ty1 element insertion upstream of the *SUF16* locus even though Ty1 mobility is only reduced to ~75% of wild type levels (Fig. 7). The interaction of Rpc37 with Ty1-IN is abolished in the *rpc53*Δ*2–280* mutant, suggesting that the Rpc53/37 subcomplex is important for targeting Ty1-IN upstream of *SUF16* (Fig. 9). Altogether our data suggest that multiple Pol III-specific subunits are able to interact with Ty1-IN to promote insertion of Ty1 elements upstream of Pol III-transcribed genes.

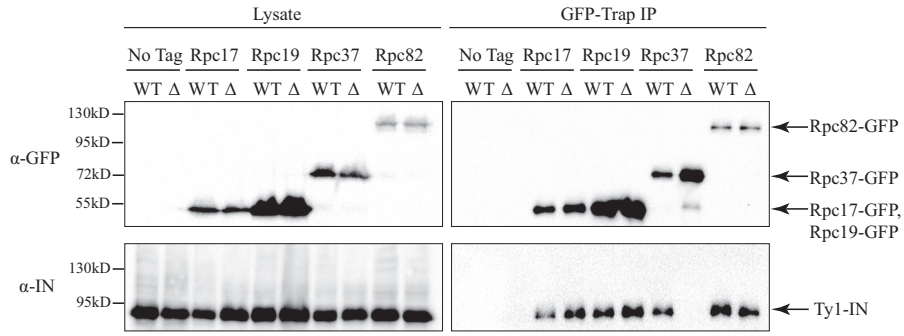

FIGURE 9. **The interaction between Ty1-IN and Rpc37 is disrupted in the *rpc53Δ2–280* mutant.** An immunoblot of whole cell lysate (*Lysate*) and GFP-Trap IP carried out from untagged (*No Tag*), Rpc17-GFP, Rpc19-GFP, Rpc37-GFP, and Rpc82-GFP cell lysates in a wild type or *rpc53Δ2–280* (Δ) strain background. Expression of a Ty1 element (*pGAL1-Ty1-H3*, pJEF724) was induced in all strains for 24 h prior to cell lysis. Immunoblots were probed with anti-GFP and anti-IN (8b11) antibodies.

To identify host proteins that interact with Ty1-IN and target the integration of Ty1 elements into the genome, we used an unbiased approach in which we purified untagged Ty1-IN using monoclonal anti-IN (8b11) antibody followed by MS analysis (27). Remarkably, about half of the proteins identified as Ty1-IN interactors in two independent purifications were subunits of RNA Pol III. Rpc25, Rpc34, Rpc40, Rpc53, and Rpc82 peptides were identified as well as the Maf1 Pol III inhibitor protein. We also identified Rpc37 and Rpc17 as candidate interactors in the first MS experiment, but these proteins were not identified in the second MS experiment. We then validated several of these interactions using an orthogonal approach in which we assessed the ability of several RNA Pol III subunits to co-immunoprecipitate with Ty1-IN. These results indicated that Ty1-IN binds to a subset of Pol III subunits but not to TFIIIB or TFIIIC subunits.

The *in vivo* and *in vitro* RNA Pol III Ty1-IN interaction data presented in this study, combined with the recently published work demonstrating an interaction between Rpc40 and Ty1-IN, begs the question of which RNA Pol III subunit(s) interact specifically with Ty1-IN (24). Our *in vitro* binding data demonstrate that at least three Pol III-specific subunits , Rpc31, Rpc34, and Rpc53, are capable of interacting with Ty1-IN (Figs. 5 and 10). Because Rpc31, Rpc34, Rpc53, and Ty1-IN were purified from *E. coli*, a post-translational modification such as phosphorylation, acetylation, or ubiquitylation is not absolutely required for these interactions to occur. It remains possible that Rpc82 is also capable of interacting directly with Ty1-IN because we were unable to purify Rpc82 to homogeneity (Fig. 5, *C* and *E*). As well, the interaction of purified $FLAG_4His_6$-Rpc128-tagged Pol III from yeast with Ty1-IN could be mediated via any of the co-purified Pol III subunits (Fig. 5, *A* and *E*). Because many of the RNA Pol III subunits interact with each other, it is possible that Ty1-IN could interact with both of the Rpc82/34/31 and Rpc53/37 subcomplexes (Fig. 10). For example, cross-linking studies have revealed that Rpc53 interacts with the Rpc82/34/31 subcomplex, the stalk, and likely the active site of Rpc160/Rpc128 (36). Although the structure of Ty1-IN has not been determined, the crystal structure of IN from the prototype foamy virus in complex with DNA, termed the prototype foamy virus intasome, revealed that prototype foamy virus IN is a homotetramer formed from two homodimers (55). Given that Ty1-IN is a 636-amino acid protein with a predicted molecular mass of 71.5 kDa, or 286kDa for a homotetramer, it is possible that Ty1-IN could interact with multiple RNA Pol III subunits.

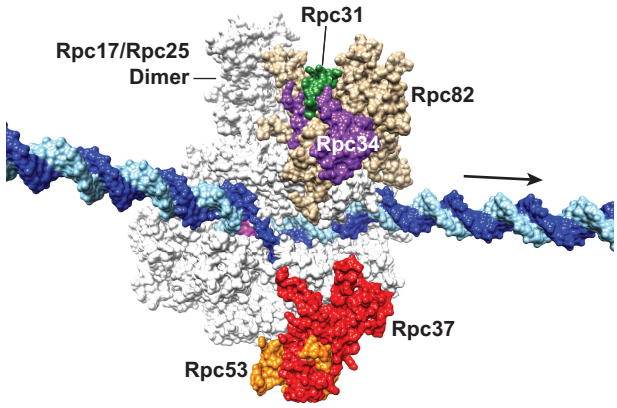

FIGURE 10. **Location of Pol III-specific subunits on a surface view of elongating Pol III.** The image is based on the cryoelectron microscopy structure of elongating Pol III (Protein Data Bank code 5FJ8) (56), and the DNA was extended based on the complete transcription bubble reported previously (75). The DNA template and non-template strands are colored in *light blue* and *dark blue*, respectively. The *arrow* points to downstream DNA, and the RNA molecule in the active site cleft is colored *magenta*. The highlighted Pol III subunits are Rpc31 (*green*), Rpc34 (*purple*), Rpc37 (*red*), Rpc53 (*orange*), and Rpc82 (*tan*). Note that the N-terminal 270 amino acids of Rpc53 are flexible and are not depicted due to the lack of structural data.

We discovered that the N-terminal 280 amino acids of Rpc53 are required for Ty1 element insertion upstream of the *SUF16* tRNA gene (Fig. 7*A*). Deletion of a short region of the Rpc53 N terminus (*rpc53Δ11–40*) reduced Ty1 element insertion upstream of *SUF16* to 50% of wild type levels (Fig. 7*A*). Interestingly, cross-linking data have shown an interaction between the N-terminal 20 amino acids of Rpc53 with Rpc25, Rpc34, and Rpc82 (36). The extended N-terminal 280 amino acids of Rpc53 cross-link to Tfc4 (TFIIIC), Rpc17, Rpc25, Rpc37, Rpc128, and Rpc160 (35, 36). A recent cryoelectron microscopy structure of RNA polymerase III suggests that the N-terminal 270 amino acids of Rpc53 are unstructured and flexible, which may explain the cross-links with multiple proteins (56). We tested whether the interaction of Ty1-IN with a selection of Pol III subunits was affected in the *rpc53Δ2–280* mutant strain. We found that the interaction between Ty1-IN and Rpc37 is abolished in the *rpc53Δ2–280* mutant, but the interaction with Rpc17, Rpc19, and Rpc82 remains intact (Fig. 9). The *in vitro*

interaction of Rpc53 with Ty1-IN, lack of Ty1 element insertion upstream of the *SUF16* locus, and loss of Ty1-IN interaction with Rpc37 in the absence of the Rpc53 N terminus strongly suggest that the Rpc53/37 subcomplex is important for targeting Ty1 elements upstream of Pol III-transcribed genes (Figs. 5, 7, 9, and 10).

Despite the lack of Ty1 element insertion upstream of *SUF16*, our Ty1 mobility assays revealed that Ty1 element mobility in the *rpc53Δ2–280* mutant occurs at a frequency of 48.2×10^{-6}, or 76% of wild type frequency (Fig. 7*B*). In the Bridier-Nahmias *et al.* (24) study, *S. cerevisiae* Rpc40 was substituted with *S. pombe* Rpc40, which no longer interacted with Ty1-IN but had a similar Ty1 retrotransposition frequency to wild type due to increased Ty1 element insertion at telomeric and subtelomeric regions. We tested whether Ty1 elements were also misdirected to telomeric regions in the *rpc53Δ2–280* mutant; however, we did not detect enrichment of Ty1 elements at these loci (Fig. 8). It will be interesting to determine where in the genome Ty1 elements are targeted in the absence of the N terminus of Rpc53.

In addition to the *rpc53Δ2–280* mutant, we identified two mutant strains, *rpc34-1* and *rpc40-V78R*, that had both highly reduced Ty1 element *SUF16* targeting and genome-wide Ty1 insertion frequency (Fig. 6, *B* and *C*). The location of the *rpc34-1* mutation is unknown, but the *rpc40-V78R* mutant likely affects the interaction with AC19/Rpc19 because overexpression of *RPC19* rescues the *rpc40-V78R* ts defect (44). As well, Rpc19 and Rpc40 interact by yeast two-hybrid analysis and based on homology to bacterial polymerase subunits are presumed to form a heterodimer (43, 44). Either Rpc34 or Rpc40 is a candidate for directly interacting with Ty1-IN, and we have demonstrated that Rpc34 and Rpc31 (both part of the Rpc82/34/31 subcomplex) are capable of interacting with Ty1-IN *in vitro* (Fig. 5*B*).

Until detailed structural analyses are performed with purified proteins, it is difficult to pinpoint precisely which Pol III subunit(s) interacts directly with Ty1-IN. Rpc82/34/31 interacts with the initiation factor TFIIIB to recruit RNA Pol III and functions in promoter opening and transcription initiation (57–64). Rpc53/37 also functions in promoter opening but has an additional role in transcription termination and reinitiation (36, 65, 66). Macromolecular MS studies have shown that both the Rpc82/34/31 and Rpc53/37 subcomplexes dissociate from the Pol III core upon perturbation of the Pol III complex with changes in pH or organic buffers (45, 46). The ability of the Rpc82/34/31 and Rpc53/37 subcomplexes to dissociate may aid in the mechanism of Ty1 element insertion, which occurs in a ~1-kbp window upstream of tRNA genes. Another remaining question is whether Ty1-IN associates with the RNA Pol III preintegration complex or the RNA Pol III complex during transcriptional elongation.

The *S. cerevisiae* Ty3/Gypsy long terminal repeat retrotransposon is also targeted upstream of Pol III-transcribed genes; however, the Ty3 element integrates precisely within a few base pairs of the Pol III transcription start site (67, 68). Ty3-IN is targeted to Pol III-transcribed genes by an interaction with TFIIIB subunits (Brf1 and TATA-binding protein/Spt15), and Ty3 element orientation depends on an interaction of Ty3-IN with TFIIIC (Tfc1) (8, 69, 70). In contrast, we found no evidence that Ty1-IN interacts with subunits of TFIIIB (Brf1 and Bfp1) or TFIIIC (Tfc1, Tfc3, and Tfc7) (Fig. 3, *B* and *C*). Our data and those of Bridier-Nahmias *et al.* (24) suggest that Ty1-IN interacts with Pol III subunits, whereas purified Pol III inhibits Ty3 element integration *in vitro* (24, 71). Another major difference between Ty1 and Ty3 element insertion is that Ty1 elements preferentially insert into nucleosomes, in particular near the H2A/H2B interface, in a periodic manner (11–14, 73). Ty1 periodic integration, but not target site specificity, requires the ISW2 chromatin remodeling complex and the N terminus of Bdp1 (15, 16). Whether or not the interaction among Ty1-IN, Pol III, and nucleosomes requires another host factor such as a chromatin-modifying complex remains to be determined. Lentiviruses such as human immunodeficiency virus type 1 preferentially integrate into active transcription units that correlate with specific histone modifications (74). Our study may imply a general mechanism for retroviral integrases to associate with RNA polymerase complexes to mediate entry into the genome of their hosts.

Author Contributions—S. C. performed and analyzed experiments in Figs. 2 and 5–9. L. M. performed and analyzed experiments in Figs. 1, 3, 4, 6, and 7. P. H. W. C. performed and analyzed experiments for Fig. 1. H.-L. H. performed protein purification for Fig. 5. T. M. helped design and analyze experiments for Fig. 1. H.-T. C. helped design and analyze experiments for Figs. 5–7 and generated Fig. 10. V. M. conceived and coordinated the study, performed experiments for Fig. 6, and wrote the paper.

Acknowledgments—We thank Joel Acker for sending us anti-RNA Pol III antibodies, Jef Boeke for the kind gift of anti-Ty1-IN antibodies and the Ty1-IN NLS and truncation constructs, and Pascale Lesage for sending us Ty1 insertion coordinates for the S. pombe AC40 mutant.

References

1. Lesage, P., and Todeschini, A. L. (2005) Happy together: the life and times of Ty retrotransposons and their hosts. *Cytogenet. Genome Res.* **110,** 70–90
2. Beauregard, A., Curcio, M. J., and Belfort, M. (2008) The take and give between retrotransposable elements and their hosts. *Annu. Rev. Genet.* **42,** 587–617
3. Curcio, M. J., Lutz, S., and Lesage, P. (2015) The Ty1 LTR-retrotransposon of budding yeast. *Microbiol. Spectr.* **3,** 1–35
4. Devine, S. E., and Boeke, J. D. (1996) Integration of the yeast retrotransposon Ty1 is targeted to regions upstream of genes transcribed by RNA polymerase III. *Genes Dev.* **10,** 620–633
5. Kim, J. M., Vanguri, S., Boeke, J. D., Gabriel, A., and Voytas, D. F. (1998) Transposable elements and genome organization: a comprehensive survey of retrotransposons revealed by the complete *Saccharomyces cerevisiae* genome sequence. *Genome Res.* **8,** 464–478
6. Qi, X., Daily, K., Nguyen, K., Wang, H., Mayhew, D., Rigor, P., Forouzan, S., Johnston, M., Mitra, R. D., Baldi, P., and Sandmeyer, S. (2012) Retrotransposon profiling of RNA polymerase III initiation sites. *Genome Res.* **22,** 681–692
7. Qi, X., and Sandmeyer, S. (2012) *In vitro* targeting of strand transfer by the Ty3 retroelement integrase. *J. Biol. Chem.* **287,** 18589–18595
8. Yieh, L., Kassavetis, G., Geiduschek, E. P., and Sandmeyer, S. B. (2000) The Brf and TATA-binding protein subunits of the RNA polymerase III transcription factor IIIB mediate position-specific integration of the gypsy-like element, *Ty3*. *J. Biol. Chem.* **275,** 29800–29807
9. Xie, W., Gai, X., Zhu, Y., Zappulla, D. C., Sternglanz, R., and Voytas, D. F.

(2001) Targeting of the yeast Ty5 retrotransposon to silent chromatin is mediated by interactions between integrase and Sir4p. *Mol. Cell. Biol.* **21,** 6606–6614
10. Zou, S., and Voytas, D. F. (1997) Silent chromatin determines target preference of the *Saccharomyces* retrotransposon Ty5. *Proc. Natl. Acad. Sci. U.S.A.* **94,** 7412–7416
11. Bachman, N., Eby, Y., and Boeke, J. D. (2004) Local definition of Ty1 target preference by long terminal repeats and clustered tRNA genes. *Genome Res.* **14,** 1232–1247
12. Baller, J. A., Gao, J., Stamenova, R., Curcio, M. J., and Voytas, D. F. (2012) A nucleosomal surface defines an integration hotspot for the *Saccharomyces cerevisiae* Ty1 retrotransposon. *Genome Res.* **22,** 704–713
13. Bridier-Nahmias, A., and Lesage, P. (2012) Two large-scale analyses of Ty1 LTR-retrotransposon *de novo* insertion events indicate that Ty1 targets nucleosomal DNA near the H2A/H2B interface. *Mob. DNA* **3,** 22
14. Mularoni, L., Zhou, Y., Bowen, T., Gangadharan, S., Wheelan, S. J., and Boeke, J. D. (2012) Retrotransposon Ty1 integration targets specifically positioned asymmetric nucleosomal DNA segments in tRNA hotspots. *Genome Res.* **22,** 693–703
15. Bachman, N., Gelbart, M. E., Tsukiyama, T., and Boeke, J. D. (2005) TFIIIB subunit Bdp1p is required for periodic integration of the Ty1 retrotransposon and targeting of Isw2p to *S. cerevisiae* tDNAs. *Genes Dev.* **19,** 955–964
16. Gelbart, M. E., Bachman, N., Delrow, J., Boeke, J. D., and Tsukiyama, T. (2005) Genome-wide identification of Isw2 chromatin-remodeling targets by localization of a catalytically inactive mutant. *Genes Dev.* **19,** 942–954
17. Curcio, M. J., Kenny, A. E., Moore, S., Garfinkel, D. J., Weintraub, M., Gamache, E. R., and Scholes, D. T. (2007) S-phase checkpoint pathways stimulate the mobility of the retrovirus-like transposon Ty1. *Mol. Cell. Biol.* **27,** 8874–8885
18. Dakshinamurthy, A., Nyswaner, K. M., Farabaugh, P. J., and Garfinkel, D. J. (2010) BUD22 affects Ty1 retrotransposition and ribosome biogenesis in *Saccharomyces cerevisiae*. *Genetics* **185,** 1193–1205
19. Griffith, J. L., Coleman, L. E., Raymond, A. S., Goodson, S. G., Pittard, W. S., Tsui, C., and Devine, S. E. (2003) Functional genomics reveals relationships between the retrovirus-like Ty1 element and its host *Saccharomyces cerevisiae*. *Genetics* **164,** 867–879
20. Risler, J. K., Kenny, A. E., Palumbo, R. J., Gamache, E. R., and Curcio, M. J. (2012) Host co-factors of the retrovirus-like transposon Ty1. *Mob. DNA* **3,** 12
21. Scholes, D. T., Banerjee, M., Bowen, B., and Curcio, M. J. (2001) Multiple regulators of Ty1 transposition in *Saccharomyces cerevisiae* have conserved roles in genome maintenance. *Genetics* **159,** 1449–1465
22. Sundararajan, A., Lee, B. S., and Garfinkel, D. J. (2003) The Rad27 (Fen-1) nuclease inhibits Ty1 mobility in *Saccharomyces cerevisiae*. *Genetics* **163,** 55–67
23. Ho, K. L., Ma, L., Cheung, S., Manhas, S., Fang, N., Wang, K., Young, B., Loewen, C., Mayor, T., and Measday, V. (2015) A role for the budding yeast separase, Esp1, in Ty1 element retrotransposition. *PLoS Genet.* **11,** e1005109
24. Bridier-Nahmias, A., Tchalikian-Cosson, A., Baller, J. A., Menouni, R., Fayol, H., Flores, A., Saib, A., Werner, M., Voytas, D. F., and Lesage, P. (2015) Retrotransposons. An RNA polymerase III subunit determines sites of retrotransposon integration. *Science* **348,** 585–588
25. Cramer, P., Armache, K. J., Baumli, S., Benkert, S., Brueckner, F., Buchen, C., Damsma, G. E., Dengl, S., Geiger, S. R., Jasiak, A. J., Jawhari, A., Jennebach, S., Kamenski, T., Kettenberger, H., Kuhn, C. D., *et al.* (2008) Structure of eukaryotic RNA polymerases. *Annu. Rev. Biophys.* **37,** 337–352
26. Longtine, M. S., McKenzie, A., 3rd, Demarini, D. J., Shah, N. G., Wach, A., Brachat, A., Philippsen, P., and Pringle, J. R. (1998) Additional modules for versatile and economical PCR-based gene deletion and modification in *Saccharomyces cerevisiae*. *Yeast* **14,** 953–961
27. Eichinger, D. J., and Boeke, J. D. (1988) The DNA intermediate in yeast Ty1 element transposition copurifies with virus-like particles: cell-free Ty1 transposition. *Cell* **54,** 955–966
28. Shevchenko, A., Tomas, H., Havlis, J., Olsen, J. V., and Mann, M. (2006) In-gel digestion for mass spectrometric characterization of proteins and proteomes. *Nat. Protoc.* **1,** 2856–2860
29. Fang, N. N., Ng, A. H., Measday, V., and Mayor, T. (2011) Hul5 HECT ubiquitin ligase plays a major role in the ubiquitylation and turnover of cytosolic misfolded proteins. *Nat. Cell Biol.* **13,** 1344–1352
30. Cox, J., Hein, M. Y., Luber, C. A., Paron, I., Nagaraj, N., and Mann, M. (2014) Accurate proteome-wide label-free quantification by delayed normalization and maximal peptide ratio extraction, termed MaxLFQ. *Mol. Cell. Proteomics* **13,** 2513–2526
31. Cox, J., and Mann, M. (2008) MaxQuant enables high peptide identification rates, individualized p.p.b.-range mass accuracies and proteome-wide protein quantification. *Nat. Biotechnol.* **26,** 1367–1372
32. Tyanova, S., Temu, T., Carlson, A., Sinitcyn, P., Mann, M., and Cox, J. (2015) Visualization of LC-MS/MS proteomics data in MaxQuant. *Proteomics* **15,** 1453–1456
33. Lannutti, B. J., Persinger, J., and Bartholomew, B. (1996) Probing the protein-DNA contacts of a yeast RNA polymerase III transcription complex in a crude extract: solid phase synthesis of DNA photoaffinity probes containing a novel photoreactive deoxycytidine analog. *Biochemistry* **35,** 9821–9831
34. Vannini, A., Ringel, R., Kusser, A. G., Berninghausen, O., Kassavetis, G. A., and Cramer, P. (2010) Molecular basis of RNA polymerase III transcription repression by Maf1. *Cell* **143,** 59–70
35. Wu, C. C., Herzog, F., Jennebach, S., Lin, Y. C., Pai, C. Y., Aebersold, R., Cramer, P., and Chen, H. T. (2012) RNA polymerase III subunit architecture and implications for open promoter complex formation. *Proc. Natl. Acad. Sci. U.S.A.* **109,** 19232–19237
36. Wu, C. C., Lin, Y. C., and Chen, H. T. (2011) The TFIIF-like Rpc37/53 dimer lies at the center of a protein network to connect TFIIIC, Bdp1, and the RNA polymerase III active center. *Mol. Cell. Biol.* **31,** 2715–2728
37. Jasiak, A. J., Armache, K. J., Martens, B., Jansen, R. P., and Cramer, P. (2006) Structural biology of RNA polymerase III: subcomplex C17/25 x-ray structure and 11 subunit enzyme model. *Mol. Cell* **23,** 71–81
38. Huet, J., Riva, M., Sentenac, A., and Fromageot, P. (1985) Yeast RNA polymerase C and its subunits. Specific antibodies as structural and functional probes. *J. Biol. Chem.* **260,** 15304–15310
39. Nyswaner, K. M., Checkley, M. A., Yi, M., Stephens, R. M., and Garfinkel, D. J. (2008) Chromatin-associated genes protect the yeast genome from Ty1 insertional mutagenesis. *Genetics* **178,** 197–214
40. Boeke, J. D., Garfinkel, D. J., Styles, C. A., and Fink, G. R. (1985) Ty elements transpose through an RNA intermediate. *Cell* **40,** 491–500
41. Carter, R., and Drouin, G. (2010) The increase in the number of subunits in eukaryotic RNA polymerase III relative to RNA polymerase II is due to the permanent recruitment of general transcription factors. *Mol. Biol. Evol.* **27,** 1035–1043
42. Huh, W. K., Falvo, J. V., Gerke, L. C., Carroll, A. S., Howson, R. W., Weissman, J. S., and O'Shea, E. K. (2003) Global analysis of protein localization in budding yeast. *Nature* **425,** 686–691
43. Flores, A., Briand, J. F., Gadal, O., Andrau, J. C., Rubbi, L., Van Mullem, V., Boschiero, C., Goussot, M., Marck, C., Carles, C., Thuriaux, P., Sentenac, A., and Werner, M. (1999) A protein-protein interaction map of yeast RNA polymerase III. *Proc. Natl. Acad. Sci. U.S.A.* **96,** 7815–7820
44. Lalo, D., Carles, C., Sentenac, A., and Thuriaux, P. (1993) Interactions between three common subunits of yeast RNA polymerases I and III. *Proc. Natl. Acad. Sci. U.S.A.* **90,** 5524–5528
45. Lane, L. A., Fernández-Tornero, C., Zhou, M., Morgner, N., Ptchelkine, D., Steuerwald, U., Politis, A., Lindner, D., Gvozdenovic, J., Gavin, A. C., Müller, C. W., and Robinson, C. V. (2011) Mass spectrometry reveals stable modules in holo and apo RNA polymerases I and III. *Structure* **19,** 90–100
46. Lorenzen, K., Vannini, A., Cramer, P., and Heck, A. J. (2007) Structural biology of RNA polymerase III: mass spectrometry elucidates subcomplex architecture. *Structure* **15,** 1237–1245
47. Acker, J., Conesa, C., and Lefebvre, O. (2013) Yeast RNA polymerase III transcription factors and effectors. *Biochim. Biophys. Acta* **1829,** 283–295
48. Cherepanov, P., Maertens, G. N., and Hare, S. (2011) Structural insights into the retroviral DNA integration apparatus. *Curr. Opin. Struct. Biol.* **21,** 249–256
49. Kenna, M. A., Brachmann, C. B., Devine, S. E., and Boeke, J. D. (1998) Invading the yeast nucleus: a nuclear localization signal at the C terminus

of Ty1 integrase is required for transposition *in vivo*. *Mol. Cell. Biol.* **18,** 1115–1124
50. Moore, S. P., Rinckel, L. A., and Garfinkel, D. J. (1998) A Ty1 integrase nuclear localization signal required for retrotransposition. *Mol. Cell. Biol.* **18,** 1105–1114
51. Panse, V. G., Hardeland, U., Werner, T., Kuster, B., and Hurt, E. (2004) A proteome-wide approach identifies sumoylated substrate proteins in yeast. *J. Biol. Chem.* **279,** 41346–41351
52. Li, Z., Vizeacoumar, F. J., Bahr, S., Li, J., Warringer, J., Vizeacoumar, F. S., Min, R., Vandersluis, B., Bellay, J., Devit, M., Fleming, J. A., Stephens, A., Haase, J., Lin, Z. Y., Baryshnikova, A., *et al.* (2011) Systematic exploration of essential yeast gene function with temperature-sensitive mutants. *Nat. Biotechnol.* **29,** 361–367
53. Ji, H., Moore, D. P., Blomberg, M. A., Braiterman, L. T., Voytas, D. F., Natsoulis, G., and Boeke, J. D. (1993) Hotspots for unselected Ty1 transposition events on yeast chromosome III are near tRNA genes and LTR sequences. *Cell* **73,** 1007–1018
54. Curcio, M. J., and Garfinkel, D. J. (1991) Single-step selection for Ty1 element retrotransposition. *Proc. Natl. Acad. Sci. U.S.A.* **88,** 936–940
55. Hare, S., Gupta, S. S., Valkov, E., Engelman, A., and Cherepanov, P. (2010) Retroviral intasome assembly and inhibition of DNA strand transfer. *Nature* **464,** 232–236
56. Hoffmann, N. A., Jakobi, A. J., Moreno-Morcillo, M., Glatt, S., Kosinski, J., Hagen, W. J., Sachse, C., and Müller, C. W. (2015) Molecular structures of unbound and transcribing RNA polymerase III. *Nature* **528,** 231–236
57. Brun, I., Sentenac, A., and Werner, M. (1997) Dual role of the C34 subunit of RNA polymerase III in transcription initiation. *EMBO J.* **16,** 5730–5741
58. Thuillier, V., Stettler, S., Sentenac, A., Thuriaux, P., and Werner, M. (1995) A mutation in the C31 subunit of *Saccharomyces cerevisiae* RNA polymerase III affects transcription initiation. *EMBO J.* **14,** 351–359
59. Wang, Z., and Roeder, R. G. (1997) Three human RNA polymerase III-specific subunits form a subcomplex with a selective function in specific transcription initiation. *Genes Dev.* **11,** 1315–1326
60. Andrau, J. C., Sentenac, A., and Werner, M. (1999) Mutagenesis of yeast TFIIIB70 reveals C-terminal residues critical for interaction with TBP and C34. *J. Mol. Biol.* **288,** 511–520
61. Bartholomew, B., Durkovich, D., Kassavetis, G. A., and Geiduschek, E. P. (1993) Orientation and topography of RNA polymerase III in transcription complexes. *Mol. Cell. Biol.* **13,** 942–952
62. Persinger, J., and Bartholomew, B. (1996) Mapping the contacts of yeast TFIIIB and RNA polymerase III at various distances from the major groove of DNA by DNA photoaffinity labeling. *J. Biol. Chem.* **271,** 33039–33046
63. Tate, J. J., Persinger, J., and Bartholomew, B. (1998) Survey of four different photoreactive moieties for DNA photoaffinity labeling of yeast RNA polymerase III transcription complexes. *Nucleic Acids Res.* **26,** 1421–1426
64. Werner, M., Chaussivert, N., Willis, I. M., and Sentenac, A. (1993) Interaction between a complex of RNA polymerase III subunits and the 70-kDa component of transcription factor IIIB. *J. Biol. Chem.* **268,** 20721–20724
65. Kassavetis, G. A., Prakash, P., and Shim, E. (2010) The C53/C37 subcomplex of RNA polymerase III lies near the active site and participates in promoter opening. *J. Biol. Chem.* **285,** 2695–2706
66. Landrieux, E., Alic, N., Ducrot, C., Acker, J., Riva, M., and Carles, C. (2006) A subcomplex of RNA polymerase III subunits involved in transcription termination and reinitiation. *EMBO J.* **25,** 118–128
67. Chalker, D. L., and Sandmeyer, S. B. (1992) Ty3 integrates within the region of RNA polymerase III transcription initiation. *Genes Dev.* **6,** 117–128
68. Sandmeyer, S., Patterson, K., and Bilanchone, V. (2015) Ty3, a position-specific retrotransposon in budding yeast. *Microbiol. Spectr.* **3,** MDNA3-0057-2014
69. Aye, M., Dildine, S. L., Claypool, J. A., Jourdain, S., and Sandmeyer, S. B. (2001) A truncation mutant of the 95-kilodalton subunit of transcription factor IIIC reveals asymmetry in Ty3 integration. *Mol. Cell. Biol.* **21,** 7839–7851
70. Yieh, L., Hatzis, H., Kassavetis, G., and Sandmeyer, S. B. (2002) Mutational analysis of the transcription factor IIIB-DNA target of Ty3 retroelement integration. *J. Biol. Chem.* **277,** 25920–25928
71. Connolly, C. M., and Sandmeyer, S. B. (1997) RNA polymerase III interferes with Ty3 integration. *FEBS Lett.* **405,** 305–311
72. Deleted in proof
73. Rinckel, L. A., and Garfinkel, D. J. (1996) Influences of histone stoichiometry on the target site preference of retrotransposons Ty1 and Ty2 in *Saccharomyces cerevisiae*. *Genetics* **142,** 761–776
74. Craigie, R., and Bushman, F. D. (2014) Host factors in retroviral integration and the selection of integration target sites. *Microbiol. Spectr.* **2,** MDNA3–0026-2014
75. Barnes, C. O., Calero, M., Malik, I., Graham, B. W., Spahr, H., Lin, G., Cohen, A. E., Brown, I. S., Zhang, Q., Pullara, F., Trakselis, M. A., Kaplan, C. D., and Calero, G. (2015) Crystal structure of a transcribing RNA polymerase II complex reveals a complete transcription bubble. *Mol. Cell* **59,** 258–269
76. Brachmann, C. B., Davies, A., Cost, G. J., Caputo, E., Li, J., Hieter, P., and Boeke, J. D. (1998) Designer deletion strains derived from *Saccharomyces cerevisiae* S288C: a useful set of strains and plasmids for PCR-mediated gene disruption and other applications. *Yeast* **14,** 115–132
77. Tong, A. H., Lesage, G., Bader, G. D., Ding, H., Xu, H., Xin, X., Young, J., Berriz, G. F., Brost, R. L., Chang, M., Chen, Y., Cheng, X., Chua, G., Friesen, H., Goldberg, D. S., *et al.* (2004) Global mapping of the yeast genetic interaction network. *Science* **303,** 808–813
78. Giaever, G., Chu, A. M., Ni, L., Connelly, C., Riles, L., Véronneau, S., Dow, S., Lucau-Danila, A., Anderson, K., André, B., Arkin, A. P., Astromoff, A., El-Bakkoury, M., Bangham, R., Benito, R., *et al.* (2002) Functional profiling of the *Saccharomyces cerevisiae* genome. *Nature* **418,** 387–391